Zone Plate Microscopy

David Attwood

University of California, Berkeley

(http://www.coe.berkeley.edu/AST/srms)

Zone Plates for Soft X-Ray Image Formation

Zone Plate Lens

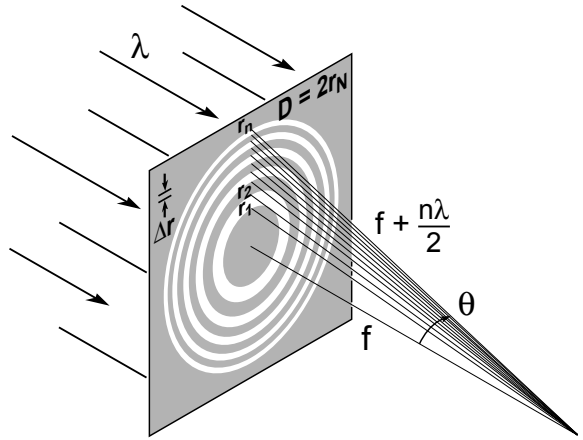

Soft X-Ray Microscope

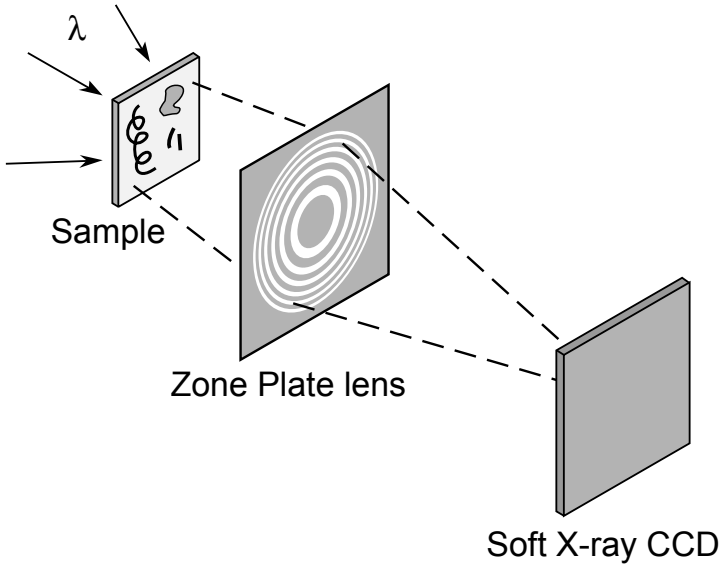

Zone Plate Formulae

$$r_n^2 = n\lambda f + \frac{n^2\lambda^2}{4} \qquad (9.9)$$

$\lambda = 2.5$ nm, $\Delta r = 25$ nm, $N = 618$

$$D = 4N\Delta r \qquad (9.13)$$

63 μm

$$f = \frac{4N(\Delta r)^2}{\lambda} \qquad (9.14)$$

0.63 mm

$$NA = \frac{\lambda}{2\Delta r} \qquad (9.15)$$

0.05 μm

$$\text{Res.} = k_1 \frac{\lambda}{\text{NA}} = 2k_1\Delta r \begin{cases} k_1 = 0.61 \\ (\sigma = 0) \end{cases} \quad 1.22\Delta r = 30 \text{ nm}$$

$$\begin{cases} k_1 = 0.4 \\ (\sigma = 0.45) \end{cases} \quad 0.8\Delta r = 19 \text{ nm}$$

$$\text{DOF} = \pm \frac{1}{2} \frac{\lambda}{(\text{NA})^2} \qquad (9.50)$$

1 μm

$$\frac{\Delta\lambda}{\lambda} \leq \frac{1}{N} \qquad (9.52)$$

1/700

Two Common Soft X-Ray Microscopes

Full-Field Microscope

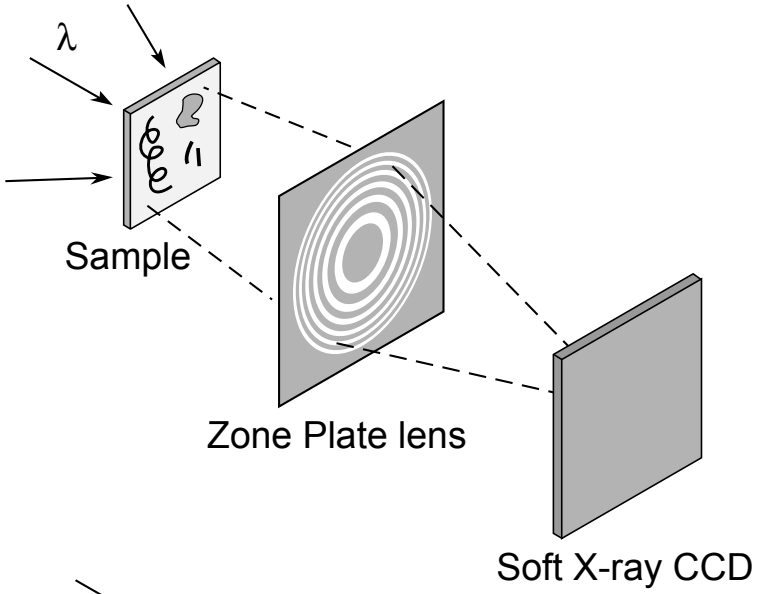

- Best spatial resolution
- Modest spectral resolution
- Shortest exposure time
- Bending magnet radiation
- Higher radiation dose
- Flexible sample environment (wet, cryo, labeled magnetic fields, electric fields, cement, ...)

Scanning Microscope

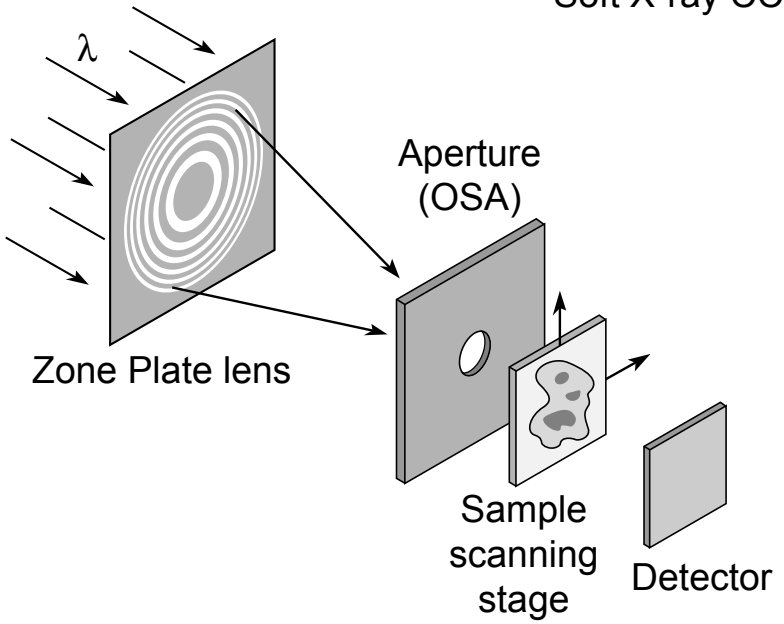

- Least radiation dose
- Next best spatial resolution
- Best spectral resolution
- Requires spatially coherent radiation
- Long exposure time
- Flexible sample environment
- Photoemission (restricted magnetic fields), fluorescence imaging

A Fresnel Zone Plate Lens for X-Ray Microscopy

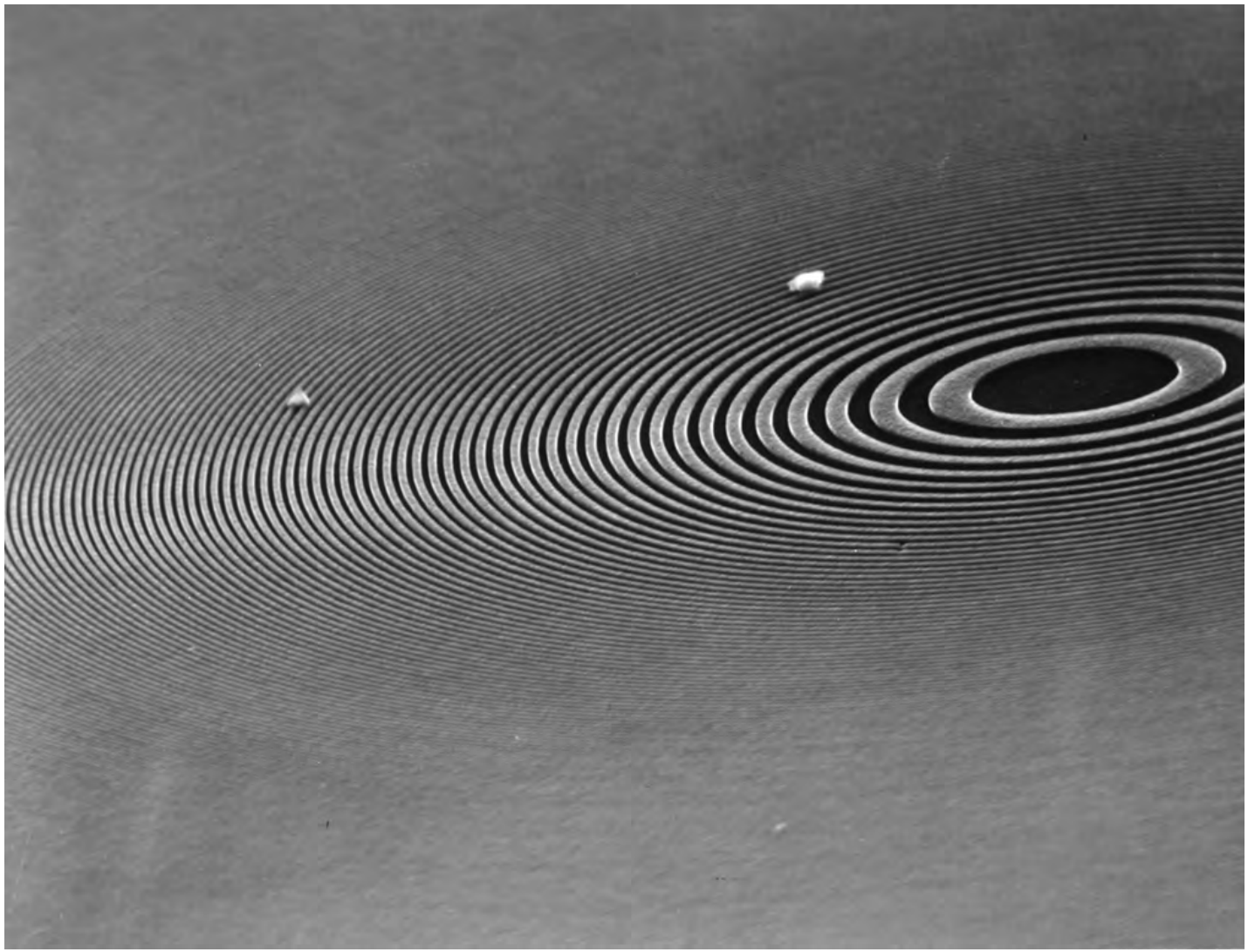

E. Anderson, LBNL

Diffraction from a Transmission Grating

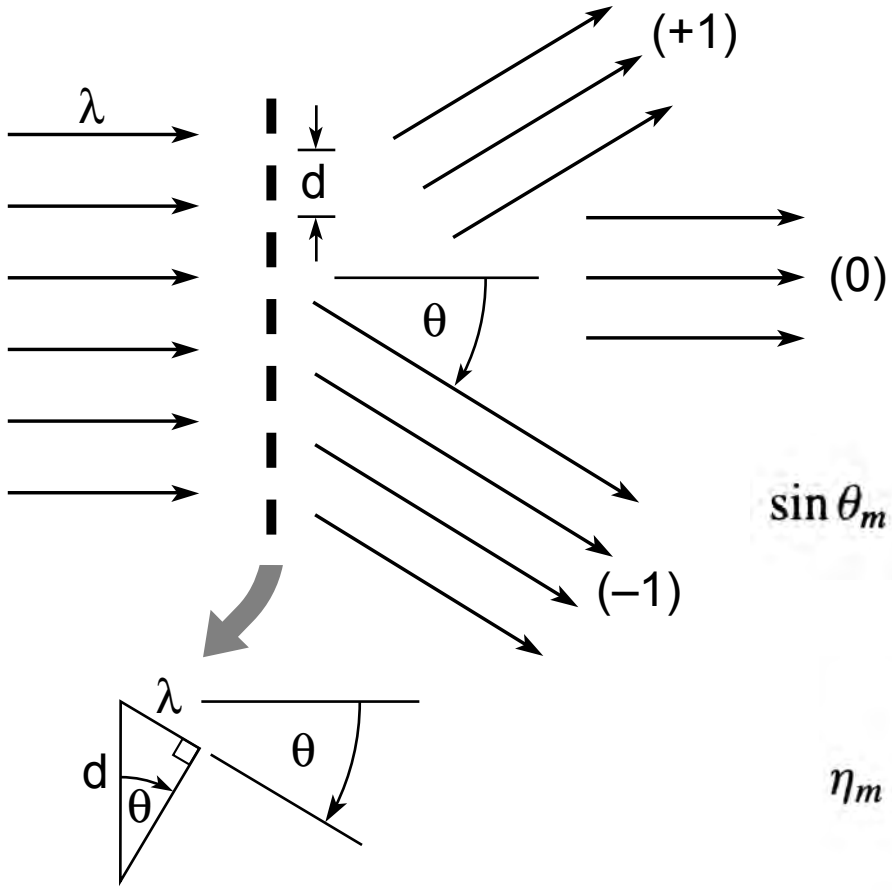

$$\sin\theta_m = \frac{m\lambda}{d}\,; \quad m = 0,\ \pm 1,\ \pm 2,\ \pm 3,\ \ldots \qquad (9.2)$$

$$\eta_m = \begin{cases} \frac{1}{4} & m = 0 \\ 1/m^2\pi^2 & m \text{ odd} \\ 0 & m \text{ even} \end{cases} \qquad (9.24)$$

(50% absorbed)

A Fresnel Zone Plate Lens

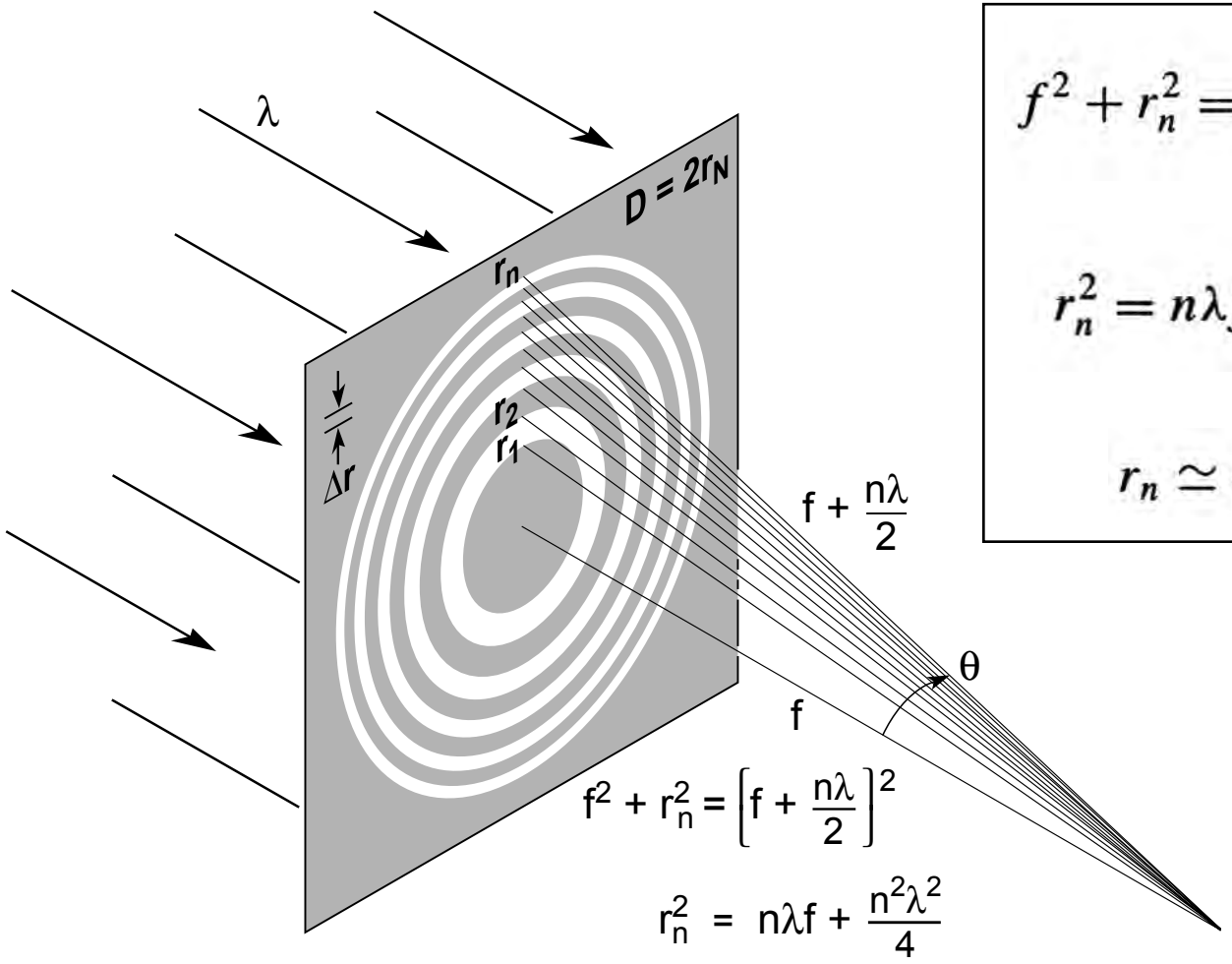

$$f^2 + r_n^2 = \left(f + \frac{n\lambda}{2}\right)^2 \qquad (9.8)$$

$$r_n^2 = n\lambda f + \frac{n^2\lambda^2}{4} \qquad (9.9)$$

$$r_n \simeq \sqrt{n\lambda f} \qquad (9.10)$$

A Fresnel Zone Plate Lens

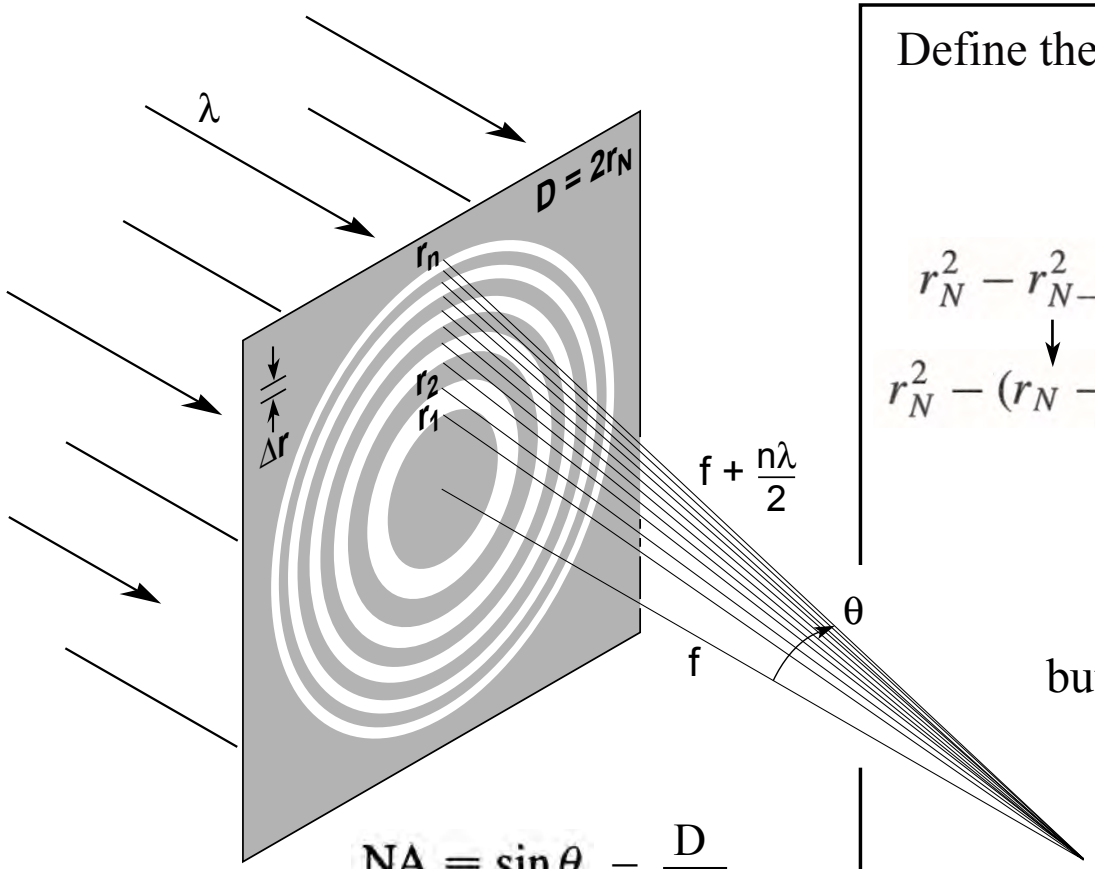

Define the outer zone width for n → N,

$$\Delta r \equiv r_N - r_{N-1} \qquad (9.11)$$

$$r_n^2 \simeq n\lambda f$$

$$r_N^2 - r_{N-1}^2 = N\lambda f - (N-1)\lambda f = \lambda f$$

$$r_N^2 - (r_N - \Delta r)^2 = 2r_N\,\Delta r - \cancel{(\Delta r)^2} \simeq 2r_N\,\Delta r$$

$$2r_N\,\Delta r \simeq \lambda f$$

$$D\,\Delta r \simeq \lambda f \qquad (9.12)$$

but $\lambda f = \dfrac{r_N^2}{N} = \dfrac{D^2}{4N}$ (from 9.10)

$$\therefore\ D\,\Delta r \simeq \frac{D^2}{4N}$$

$$\boxed{D \simeq 4N\,\Delta r} \qquad (9.13)$$

and from (9.12) above

$$\boxed{f \simeq \frac{4N(\Delta r)^2}{\lambda}} \qquad (9.14)$$

$$\mathrm{NA} \equiv \sin\theta = \frac{D}{2f}$$

$$\mathrm{NA} \simeq \frac{\lambda}{2\,\Delta r} \qquad (9.15)$$

$$F^{\#} \equiv \frac{f}{D} \simeq \frac{\Delta r}{\lambda} \qquad (9.16)$$

A Fresnel Zone Plate Lens Used as a Diffractive Lens for Point to Point Imaging

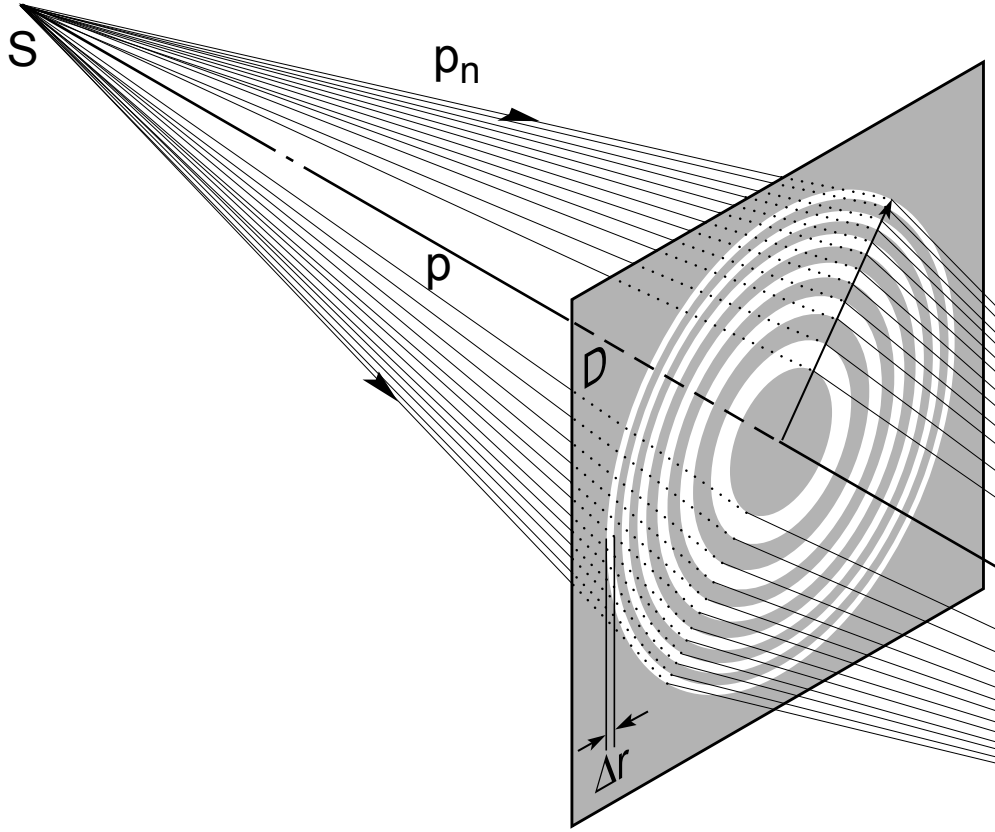

$$q_n + p_n = q + p + \frac{n\lambda}{2}$$

$$q_n = (q^2 + r_n^2)^{1/2} \simeq q + \frac{r_n^2}{2q}$$

$$p_n = (p^2 + r_n^2)^{1/2} \simeq p + \frac{r_n^2}{2p}$$

$$\cancel{q} + \frac{r_n^2}{2q} + \cancel{p} + \frac{r_n^2}{2p} \simeq \cancel{q} + \cancel{p} + \frac{n\lambda}{2}$$

$$\frac{1}{q} + \frac{1}{p} \simeq \frac{n\lambda}{r_n^2}$$

$$\boxed{\frac{1}{q} + \frac{1}{p} \simeq \frac{1}{f}} \quad (9.17)$$

$$\boxed{M = \frac{p}{q}} \quad (9.18)$$

Zone Plate Diffractive Focusing for Higher Orders

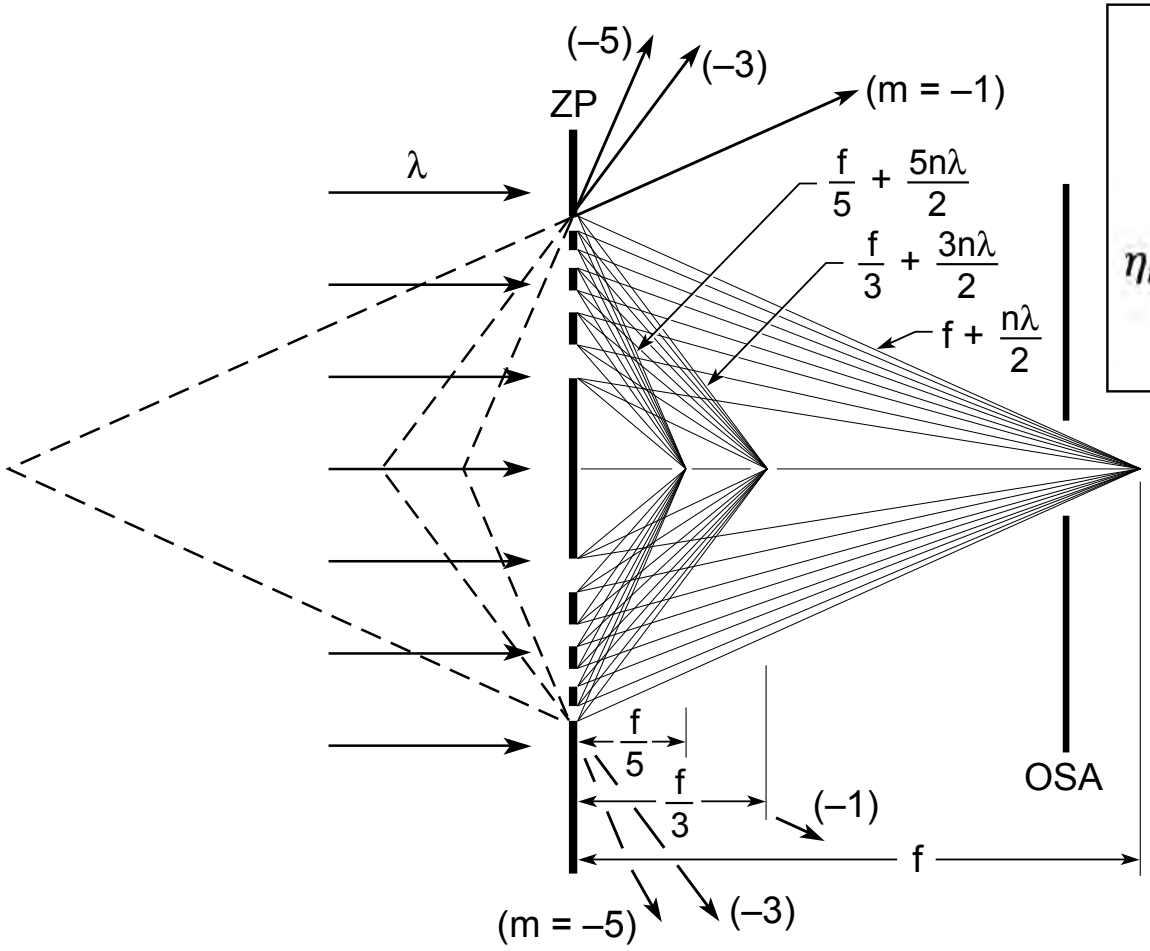

$$r_n^2 \simeq mn\lambda f_m \qquad (9.19)$$

$$\eta_m = \begin{cases} \frac{1}{4} & m = 0 \\ 1/m^2\pi^2 & m \text{ odd} \\ 0 & m \text{ even} \end{cases} \qquad (9.24)$$

$$f_m = \frac{1}{m}\,\frac{r_N^2}{N\lambda}$$

$$f_m = \frac{1}{m}\,f_1$$

Diffraction from a Fresnel Zone Plate

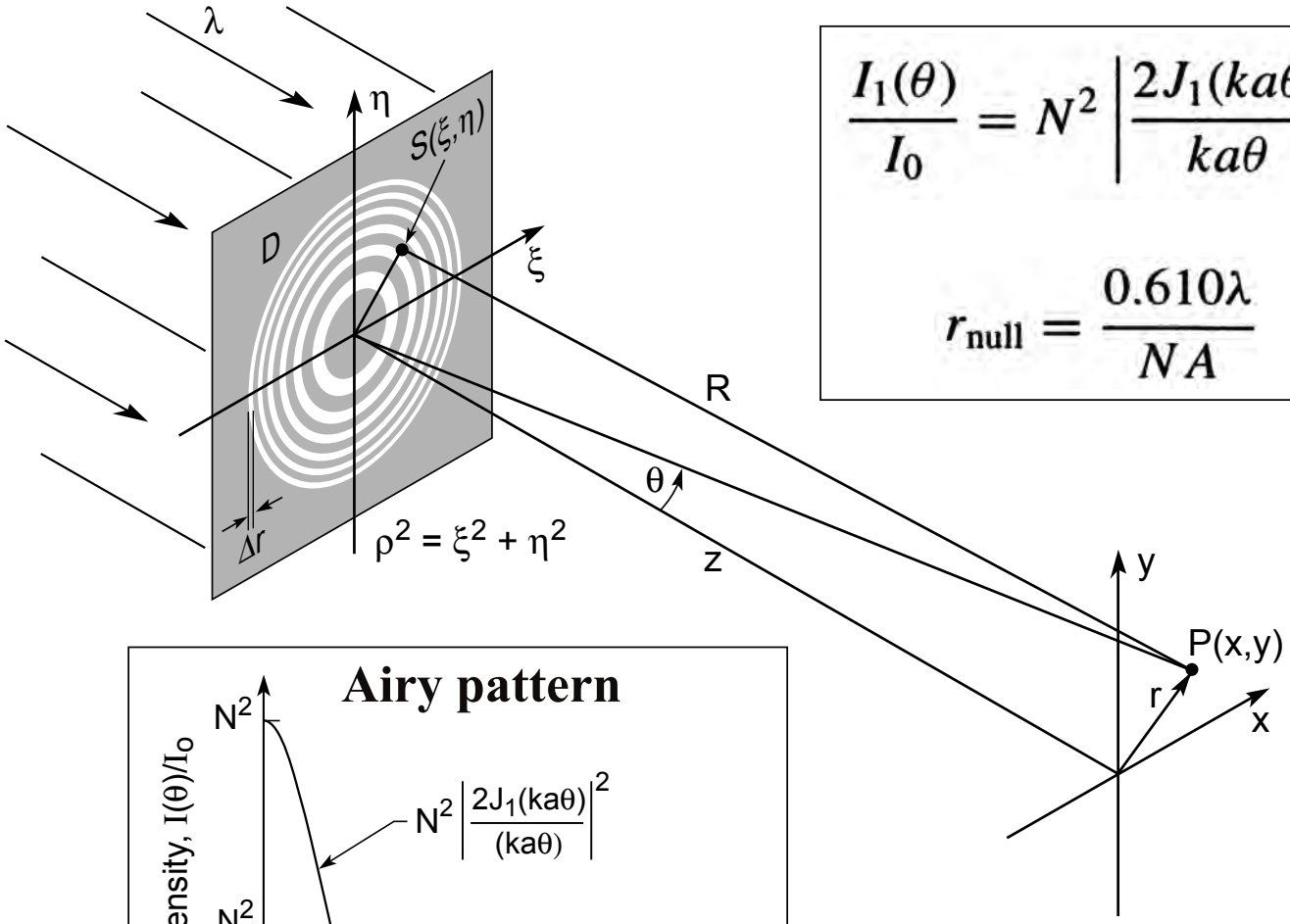

$$\frac{I_1(\theta)}{I_0} = N^2 \left| \frac{2J_1(ka\theta)}{ka\theta} \right|^2 \qquad (9.45)$$

$$r_{\text{null}} = \frac{0.610\lambda}{NA} \qquad (9.46)$$

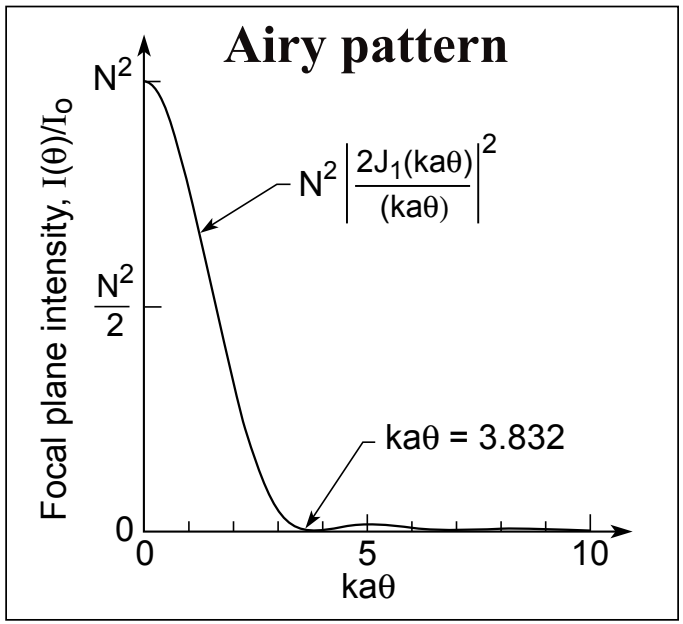

Resolving Two Point Sources

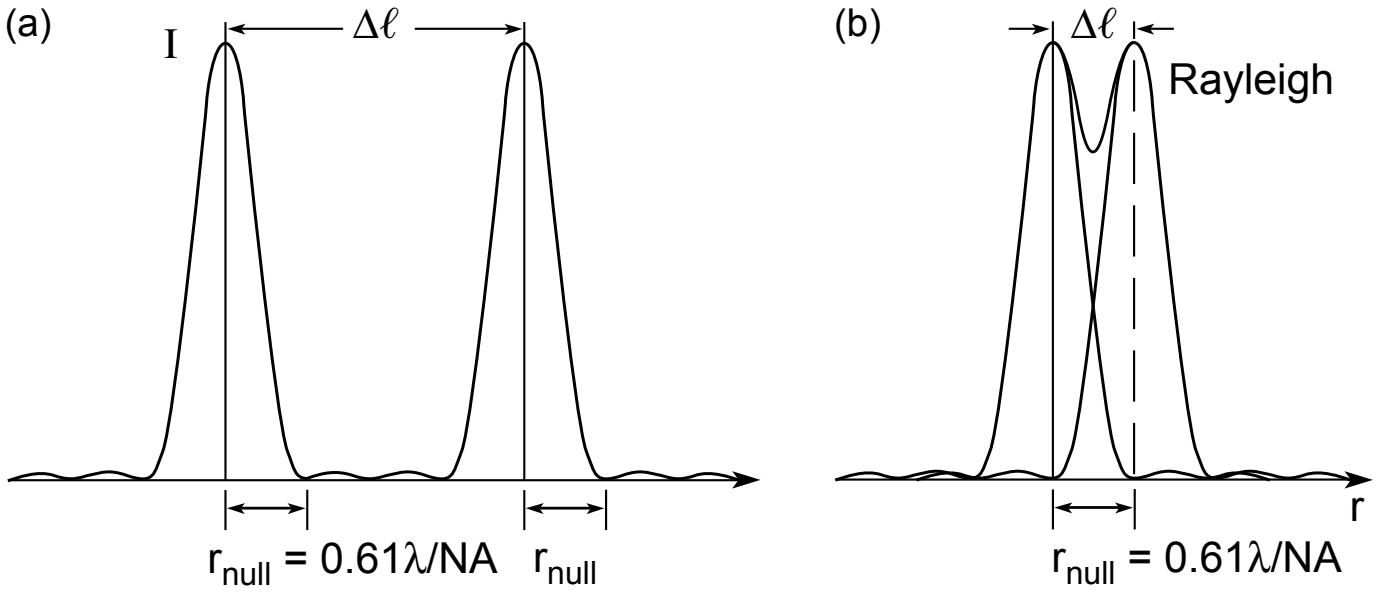

- Point sources are spatially coherent
- Mutually incoherent
- Intensities add
- Rayleigh criterion (26.5% dip)

Conclusion: With spatially coherent illumination, objects are "just resolvable" when

$$\text{Res}|_{\text{coh}} = \frac{0.61\,\lambda}{\text{NA}} = 1.22\,\Delta r$$

Fresnel Zone Plate Lens for Diffractive Focusing of Spatially Coherent X-rays

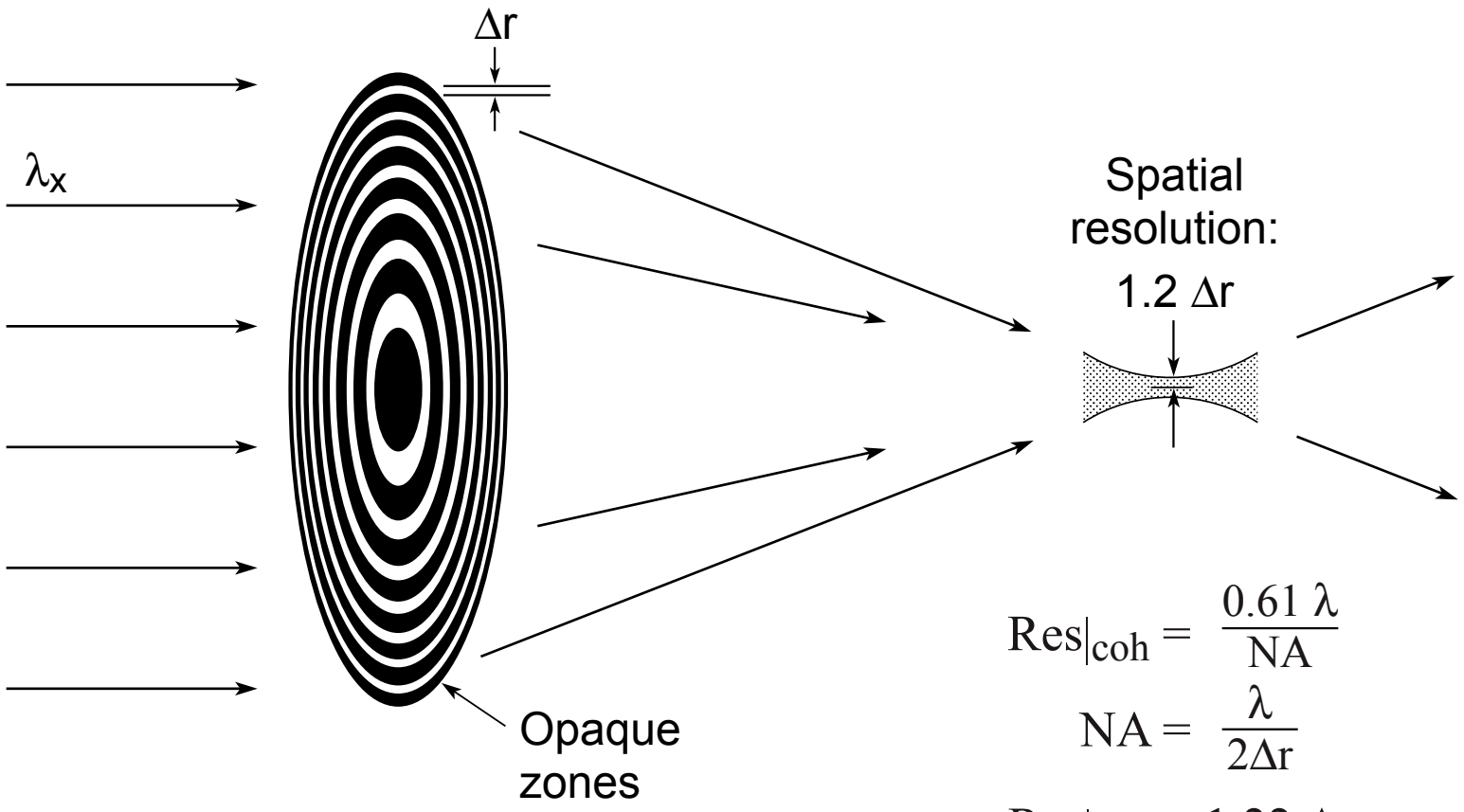

$$\text{Res}|_{coh} = \frac{0.61\,\lambda}{NA}$$

$$NA = \frac{\lambda}{2\Delta r}$$

$$\therefore \text{Res}|_{coh} = 1.22\,\Delta r$$

Coherent illumination
($\sigma = 0$)

($\sigma = 0$, see first slide)

Partially Coherent Illumination Permits Improved Spatial Resolution by a Factor Approaching Two

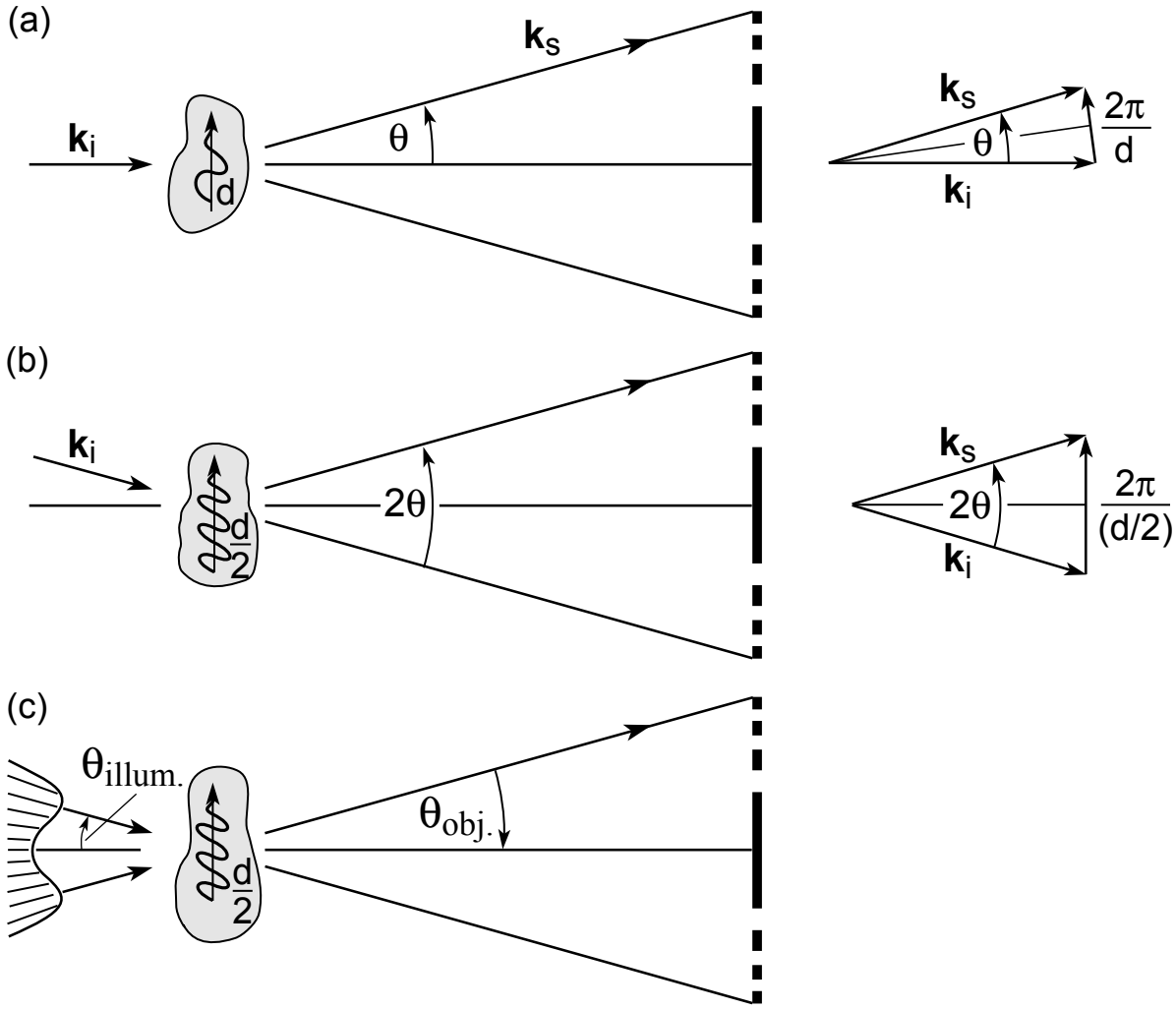

$$\sigma \equiv \frac{NA_{illum.}}{NA_{obj.}} = \frac{\sin\theta_{illum.}}{\sin\theta_{obj.}} \quad (\text{for } n = 1)$$

Optical Transfer Properties with Varying Degrees of Partially Coherent Illumination

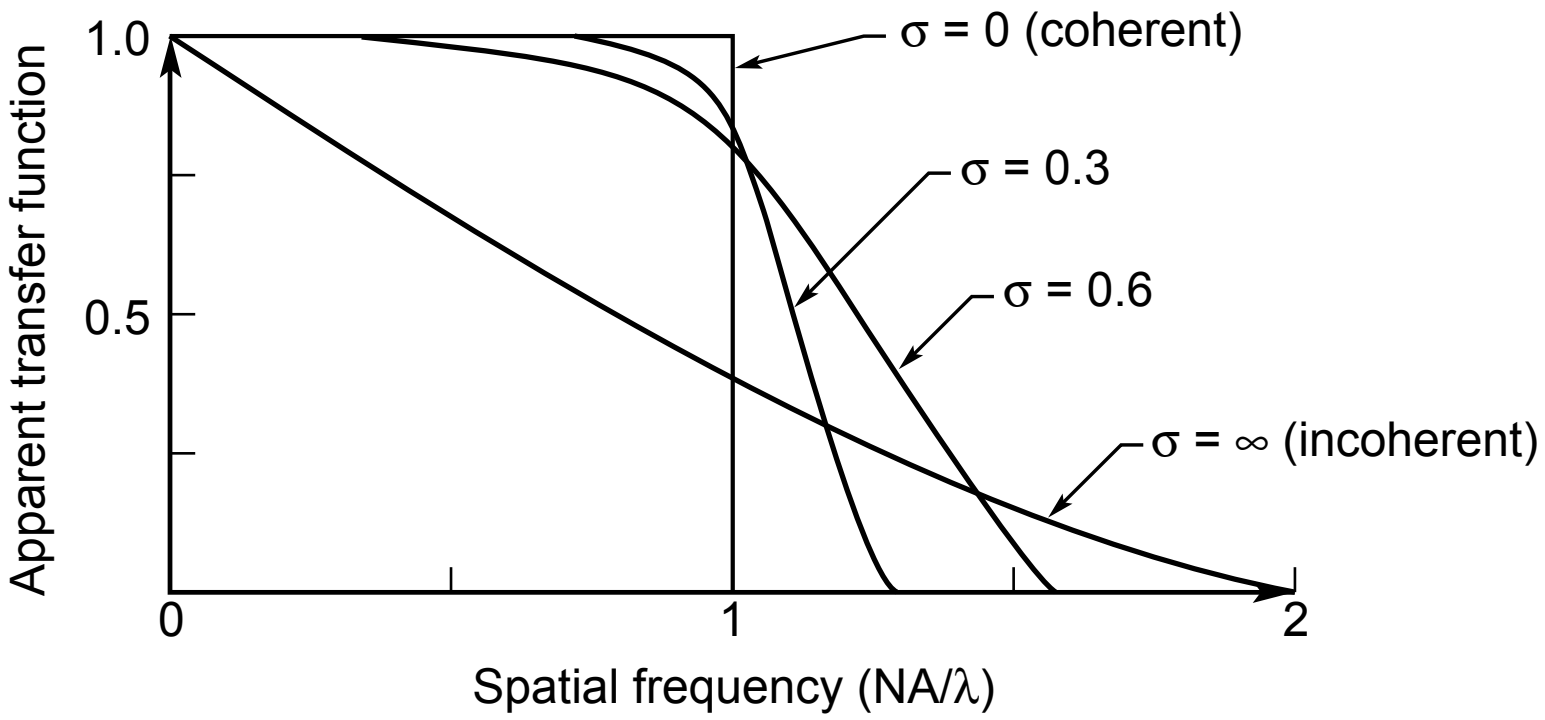

$$\sigma \equiv \frac{NA_{illum.}}{NA_{obj.}} = \frac{\sin\theta_{illum.}}{\sin\theta_{obj.}} \quad (\text{for } n = 1)$$

Intensity Versus Position for a Sharp Edge Observed With Coherent and Partially Coherent Radiation

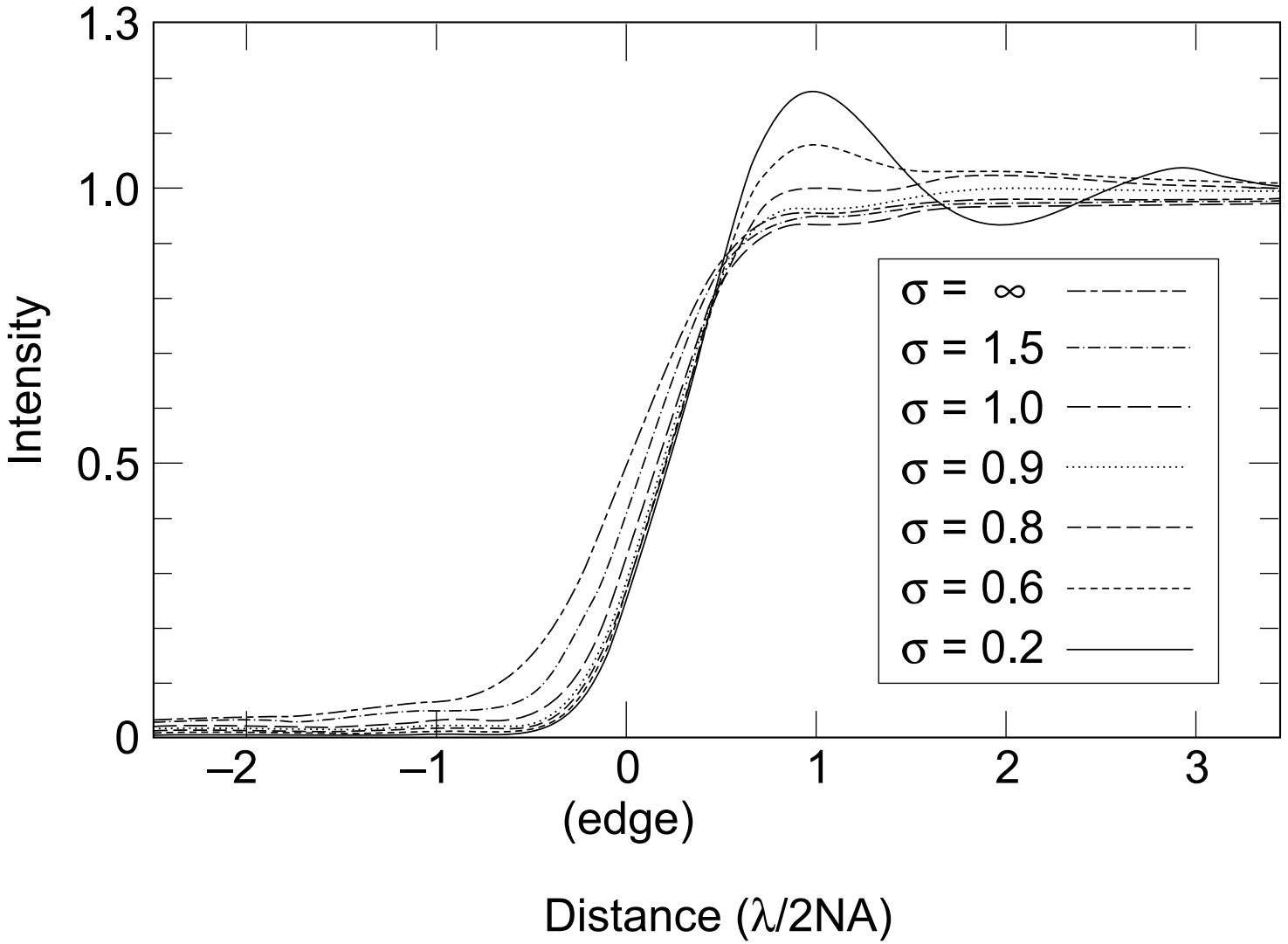

Courtesy of M. O'Toole and A. Neureuther (UC Berkeley).

Depth of Focus and Spectral Bandwidth

$$\Delta z = \pm \frac{1}{2} \frac{\lambda}{(\mathrm{NA})^2} \qquad (9.50)$$

$$\Delta z = \pm 2F^{\#2}\lambda = \pm 2(\Delta r)^2/\lambda \qquad (9.51)$$

$$\frac{\Delta\lambda}{\lambda} \leq \frac{1}{N} \qquad (9.52)$$

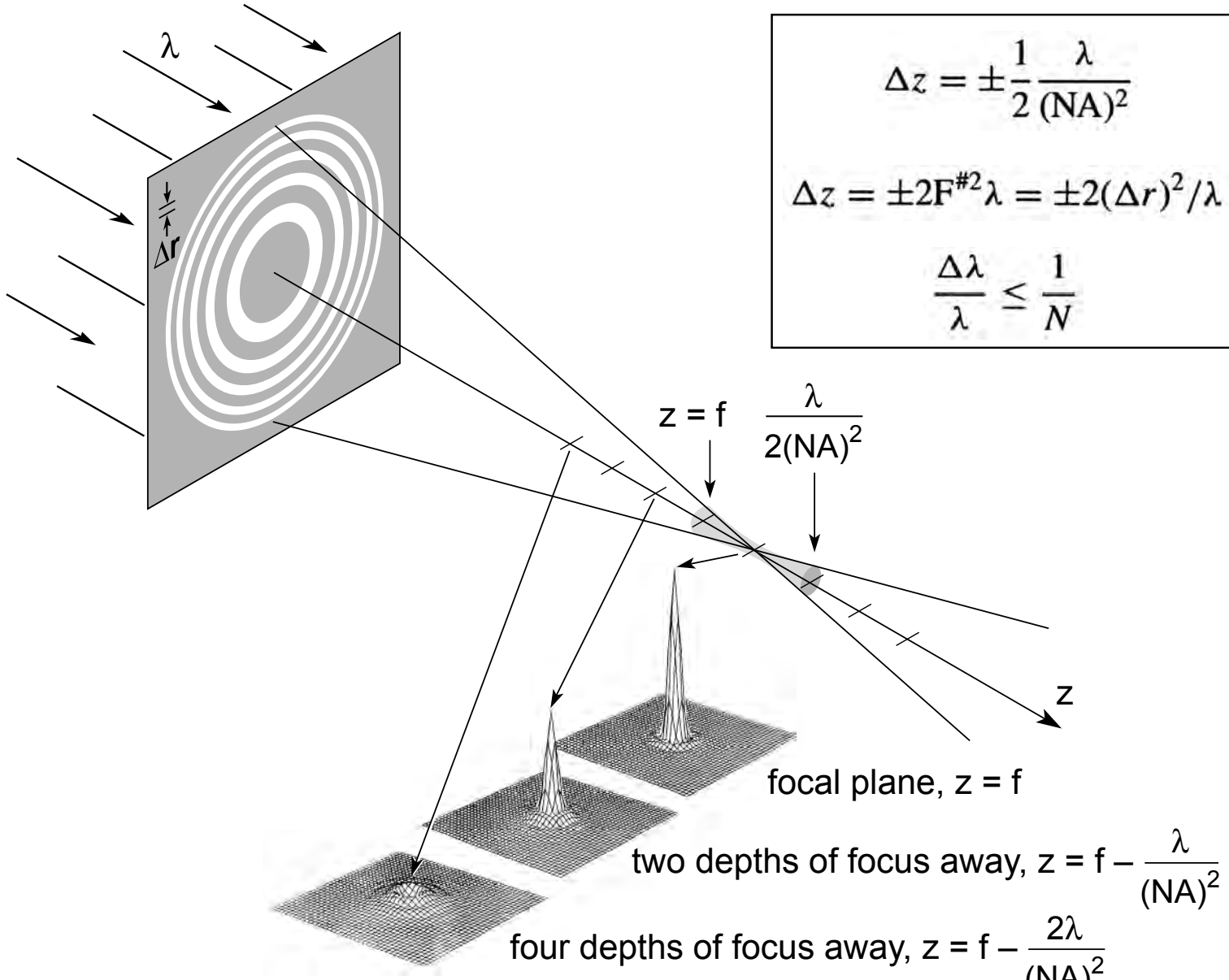

Why does DOF Scale as λ/NA2?

High NA

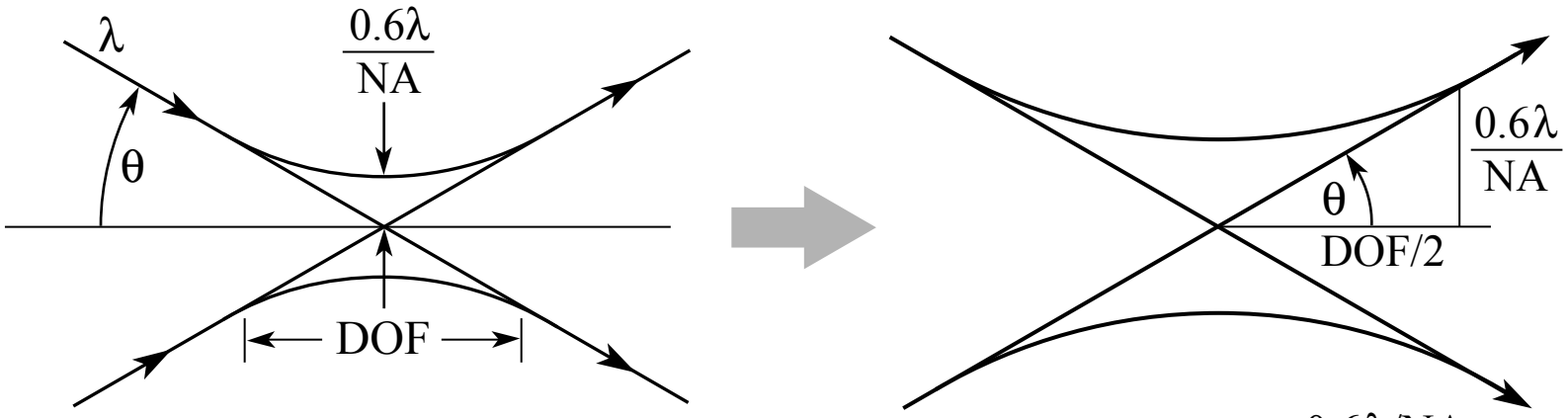

$$\tan\theta = \frac{0.6\lambda/NA}{DOF/2}$$

$$DOF = \frac{1.2\lambda/NA}{\tan\theta}$$

Low NA

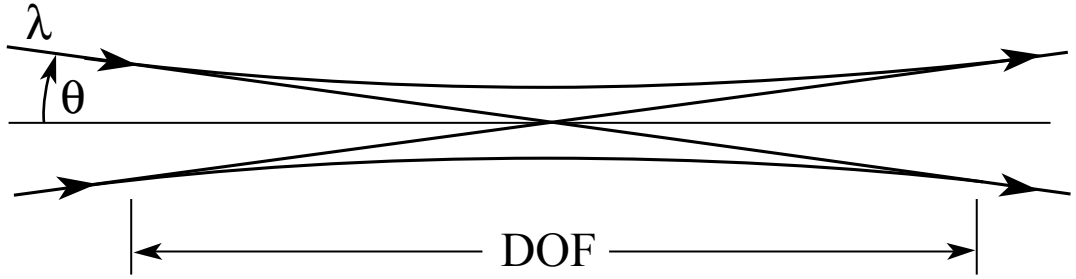

for small θ

$$\tan\theta \sim \sin\theta = NA$$

$$\therefore DOF \simeq \frac{1.2\lambda}{NA^2}$$

in the text, eq. 9.50:

$$DOF = \pm \frac{1}{2} \frac{\lambda}{(NA)^2}$$

Test Pattern for Nanometer Soft X-ray Imaging

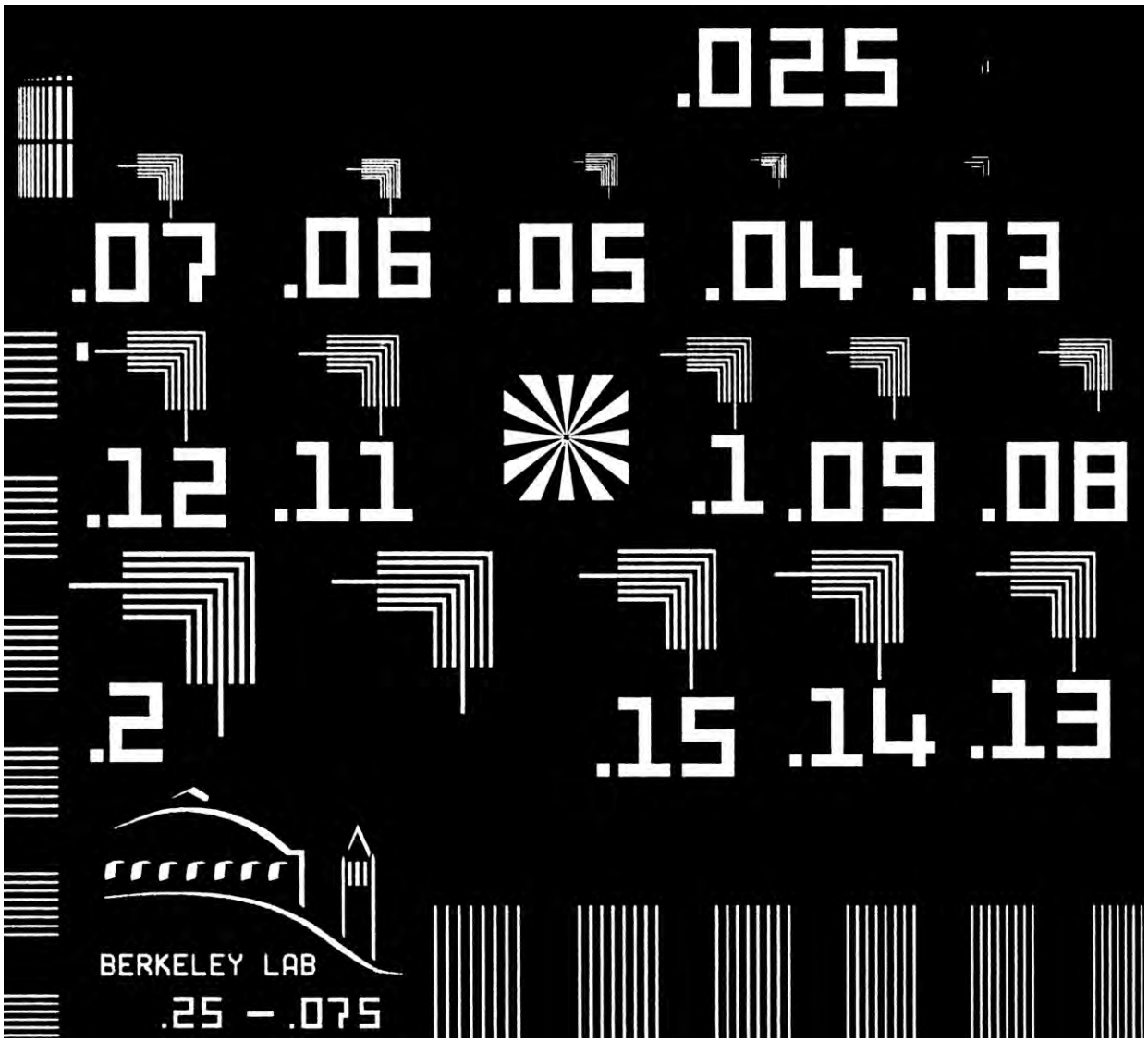

E. Anderson, D. Olynick, B. Harteneck, E. Veklerov, LBNL

The XM-1 Soft X-Ray Microscope at the Advanced Light Source (ALS)

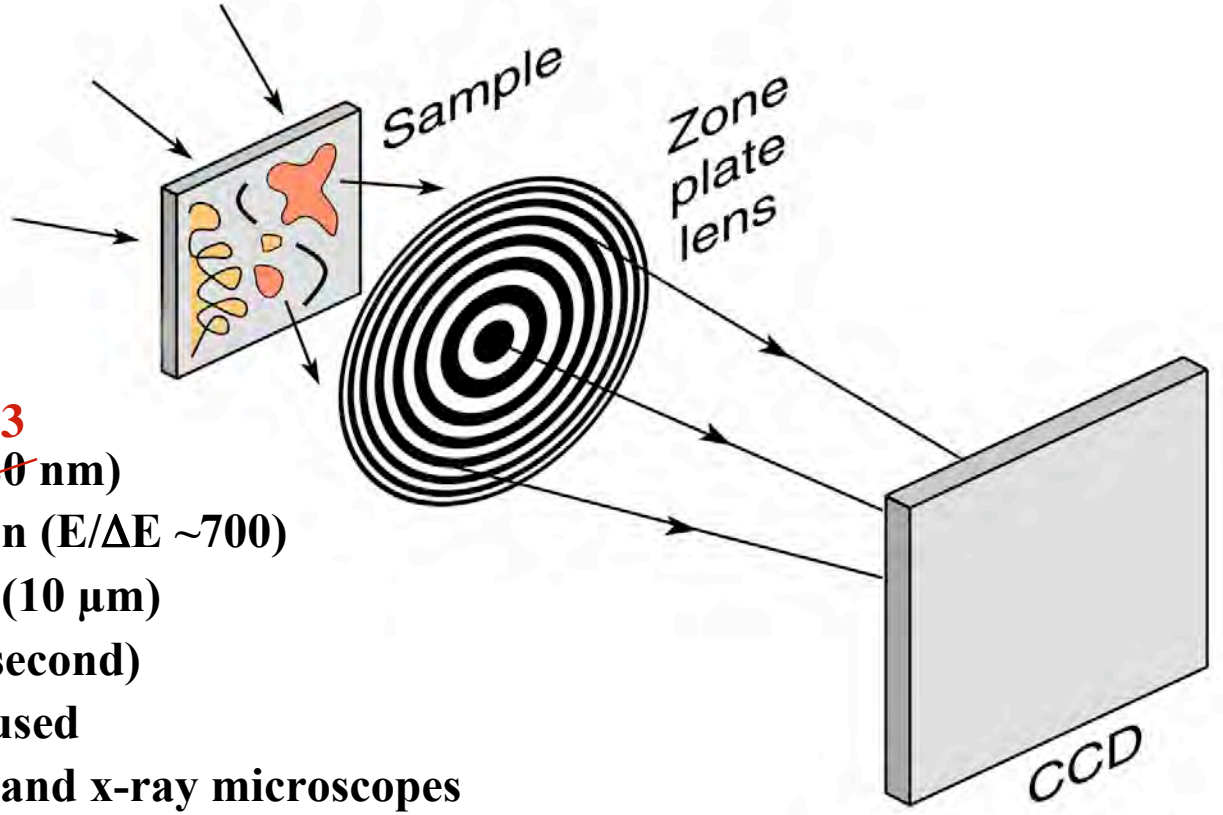

- High spatial resolution (~~20~~ 13 nm)
- Modest spectral resolution (E/ΔE ~700)
- Thick, hydrated samples (10 μm)
- Short exposure time (~1 second)
- Well engineered, pre-focused
- Mutually indexed visible and x-ray microscopes
- High throughput (hundreds of samples per day)
- Large image fields by tiling
- Easy access, user friendly
- Cryotomography

E = 250 - 1.8 keV
λ = 0.7 nm - 5 nm

High Resolution Zone-Plate Microscope XM-1 at the ALS

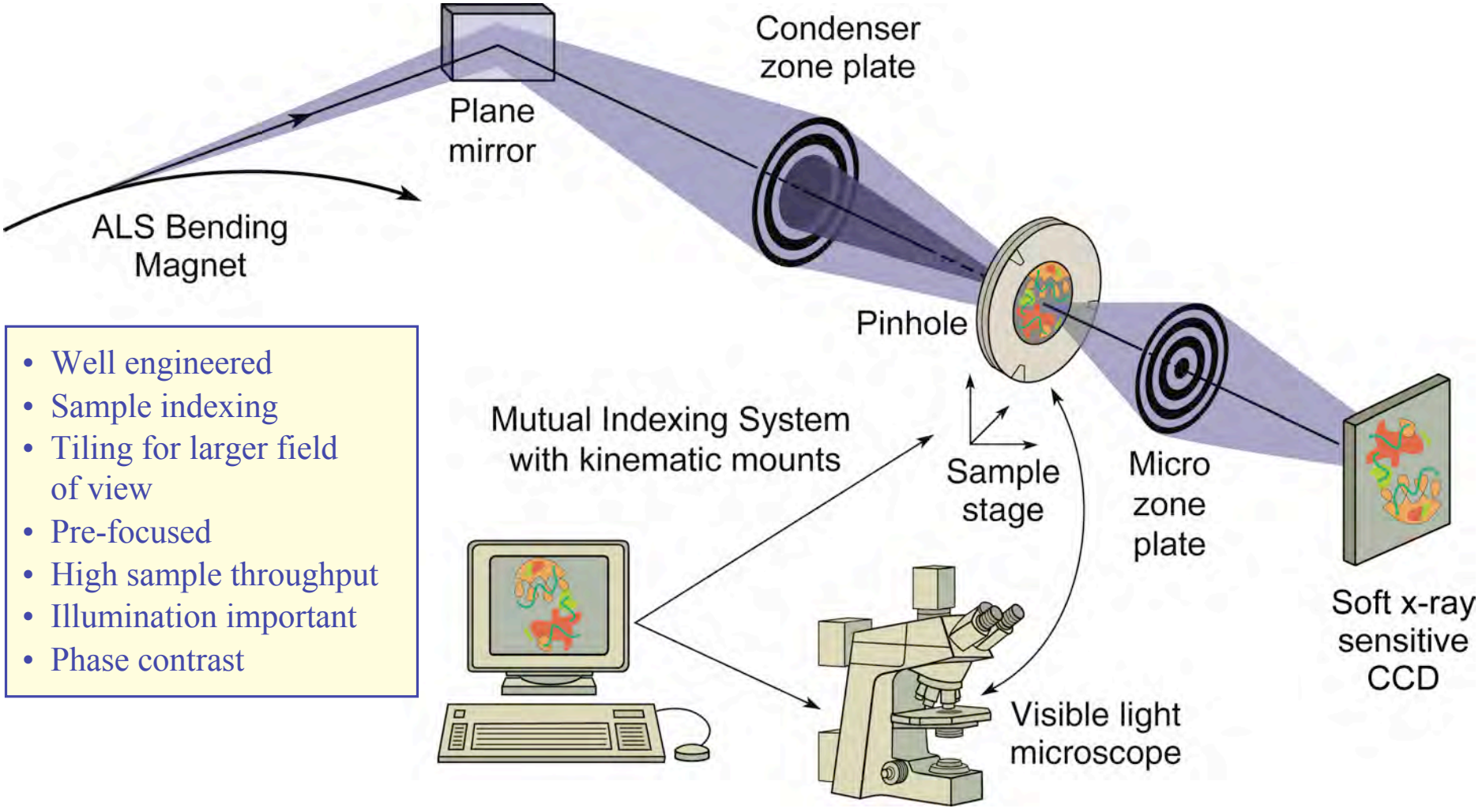

- Well engineered
- Sample indexing
- Tiling for larger field of view
- Pre-focused
- High sample throughput
- Illumination important
- Phase contrast

Bending Magnet Photon Flux at the ALS

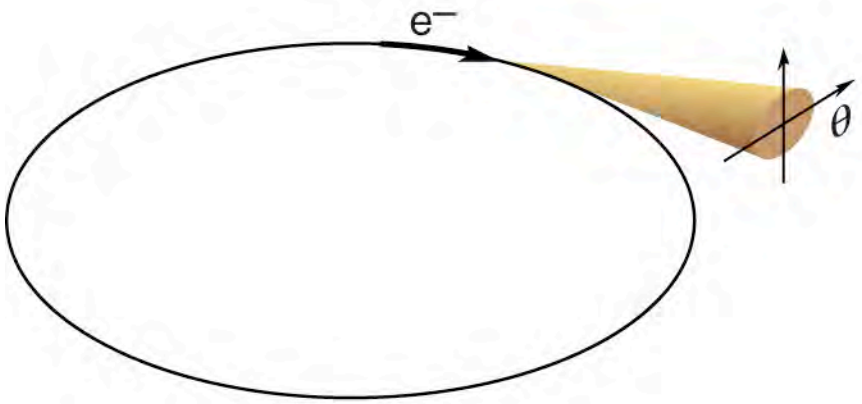

$$E_c = \hbar\omega_c = \frac{3e\hbar B\gamma^2}{2m} \qquad (5.7a)$$

$$E_c(\text{keV}) = 0.6650 E_e^2(\text{GeV}) B(\text{T}) \qquad (5.7b)$$

$$\gamma = \frac{E_e}{mc^2} = 1957 E_e(\text{GeV}) \qquad (5.5)$$

Advantages:
- covers broad spectral range
- least expensive
- most accessable

Disadvantages:
- limited coverage of hard x-rays
- not as bright as undulator

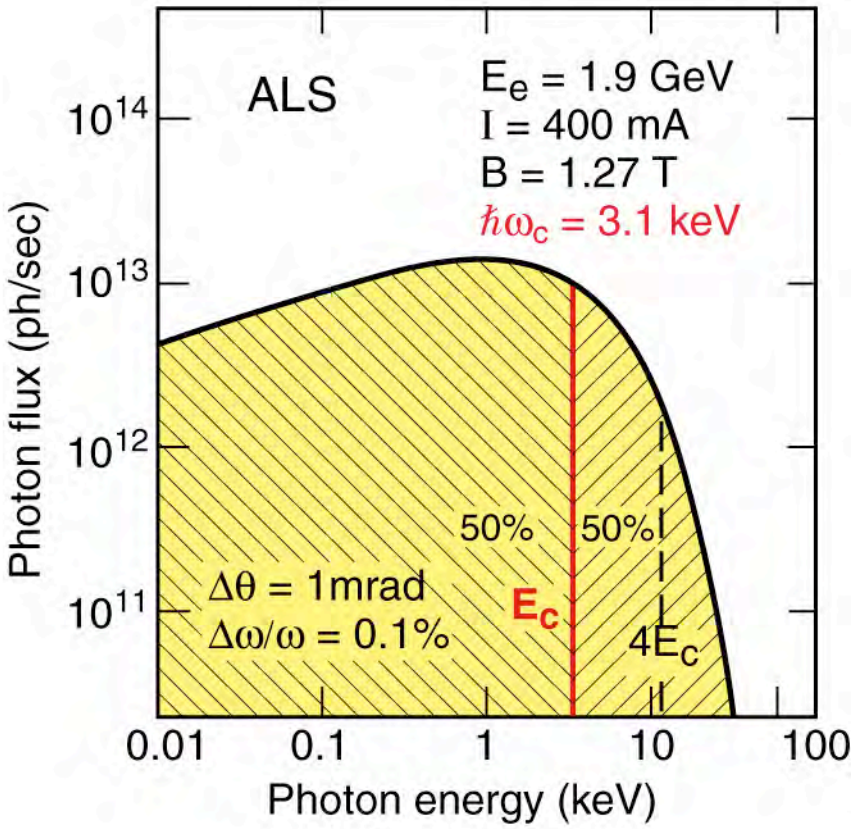

XM-1 Parameters

Micro Zone Plates

Δr = 25 nm (15 nm), Δt = 70 nm (5%) (170 nm). N = 618, D = 63 μm, f = 650 μm, NA = 0.05 at 2.4 nm. Δr = 35 nm, Δt = 85 nm (8%).

Condenser Zone Plate

Δr = 55 nm (40 nm), Δt = 200 nm (22%). N = 41,000, D = 9 mm, f = 207 mm, NA = 0.022 @ 2.4 nm. σ = 0.45 with Δr = 25 nm micro zone plate.

Magnification

M = 2400 to 3100; 24 μm CCD pixel → 8 nm at sample.

Spectral Bandpass

$\lambda/\Delta\lambda$ = 700, per pixel, 2 μm^D field.
$\lambda/\Delta\lambda$ = 500 with shaker, 10 μm^D field.

CCD Camera

Back thinned, soft x-ray sensitive. 1024 x 1024 (2048 x 2048), 24 μm square pixels. 60 -70% efficient.

Exposure Time

1-5 seconds, 10^3 photons/pixel, 8 μm diameter at sample (2.5 sec @ 400 mA, 2 x 2 binning, Δr = 25 nm)

New Overlay Nanofabrication Technique for Narrower Outer Zones

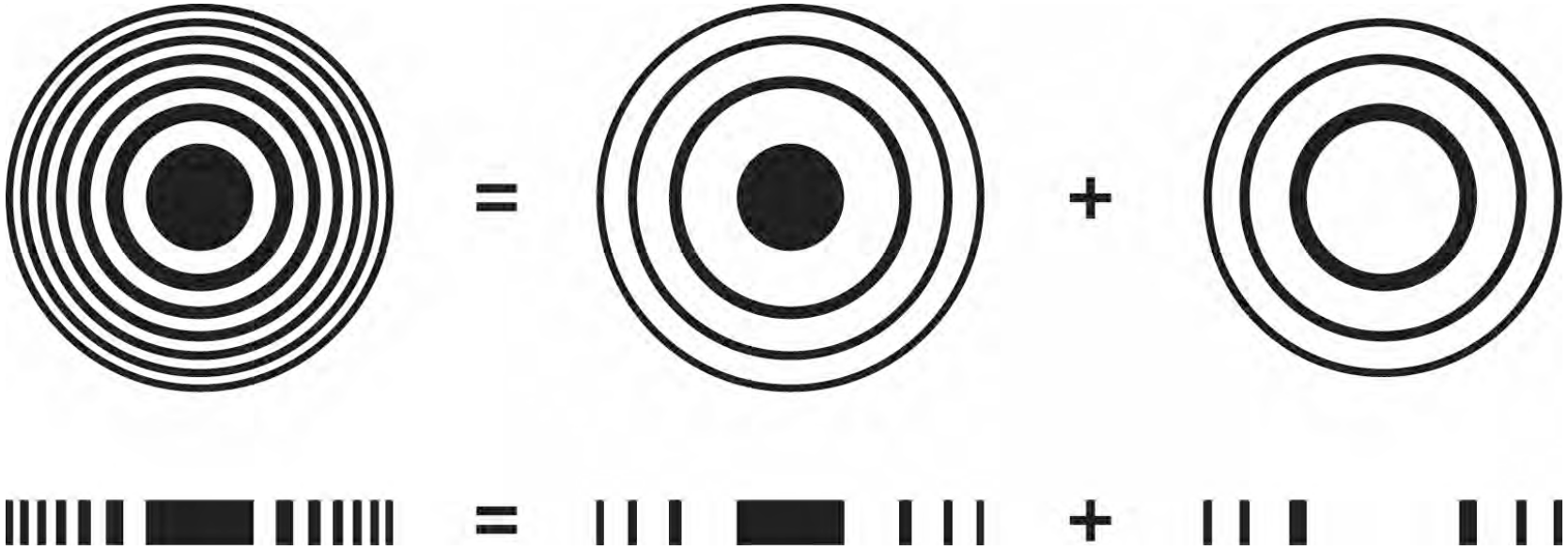

$\Delta r = 15$ nm

$\Delta t = 90$ nm

Overlay $\simeq$ 2 nm accuracy

Courtesy of J.A. Liddle, E.H. Anderson, B. Harteneck and W. Chao, LBNL

Multilayer Mirror Coatings Can Be Thinned and Used As Sub-20 nm Test Patterns

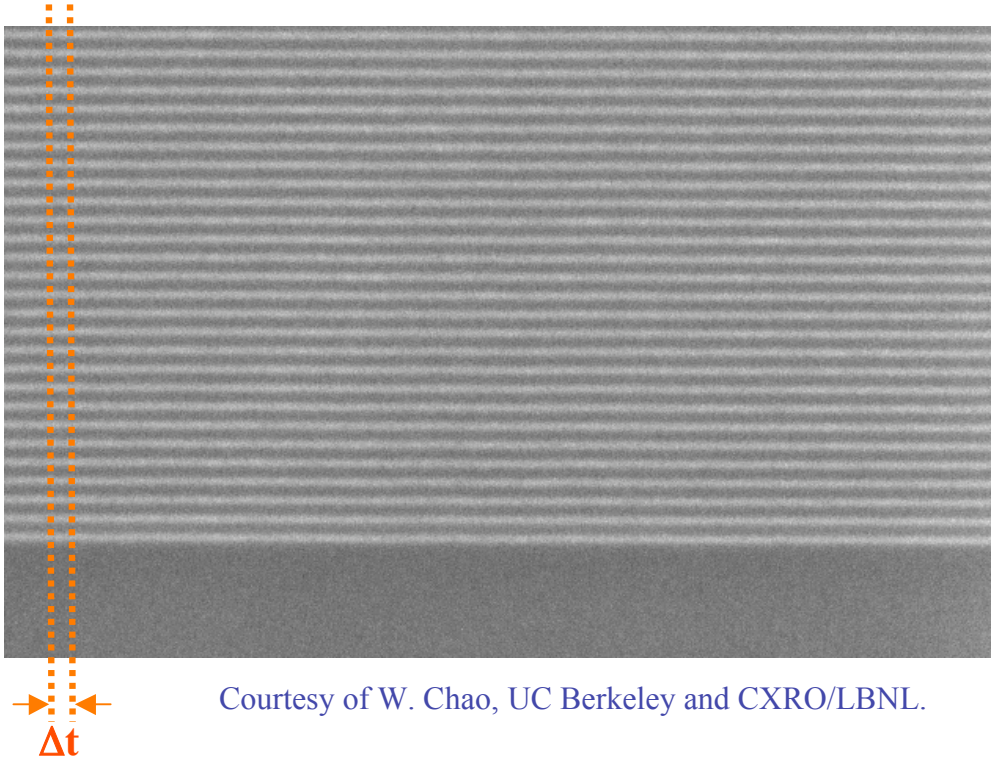

Courtesy of W. Chao, UC Berkeley and CXRO/LBNL.

SEM Micrograph
of Cr/Si test pattern

High quality test patterns can be fabricated with sections as thin as 5 nm.

Near Diffraction Limited Soft X-Ray Microscopy: 20 nm Spatial Resolution at 2.07 nm Wavelength

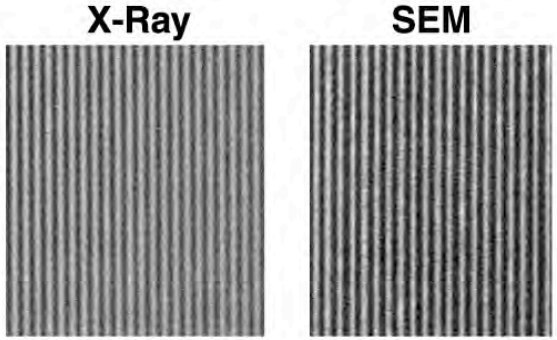

24 nm lines and spaces (Cr/Si)
75% modulation
600 eV (2.07 nm)

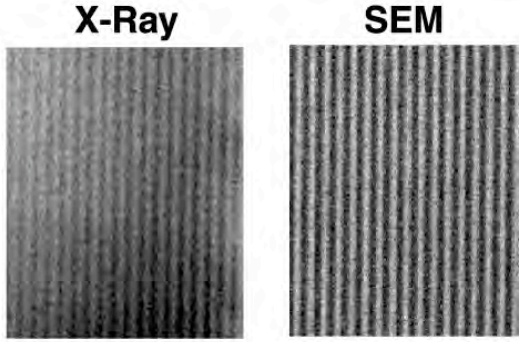

19 nm lines and spaces (Cr/Si)
20% modulation (barely "resolved")

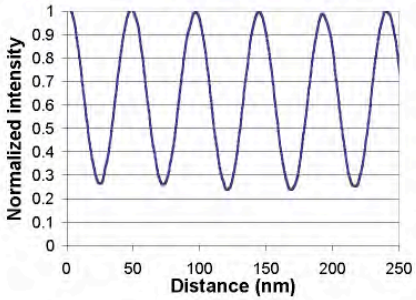

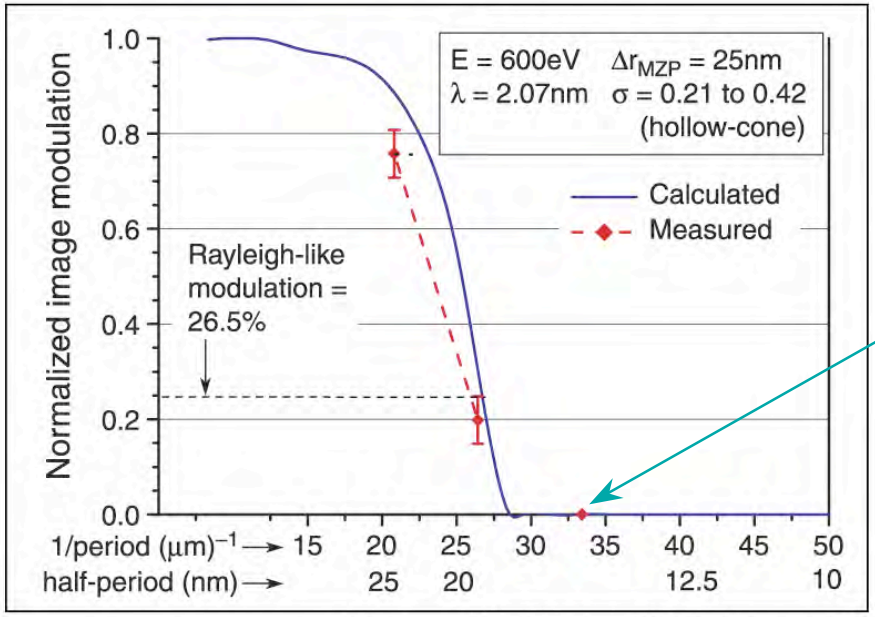

15 nm lines
not resolved,
no modulation

(Courtesy of Weilun Chao, UC Berkeley and CXRO/LBNL)

W. Chao et al.,
Opt. Lett. 28, 2019 (Nov 2003)

New Results Using Overlay Nanofabrication: Outer Zone Width of 15 nm

- Zone plate lenses made using a new, e-beam based nanofabrication technique have extended outer zones from 25 nm to 15 nm.
- The new lenses work as expected, resolving fine patterns not seen previously
- Shorter depth of focus (λ/NA^2) opens the opportunity for soft x-ray "optical sectioning" of biological material.

New zone plate lens with 15 nm outer zone width

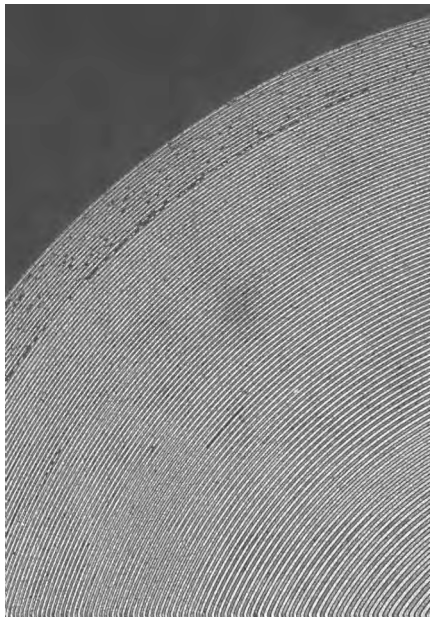

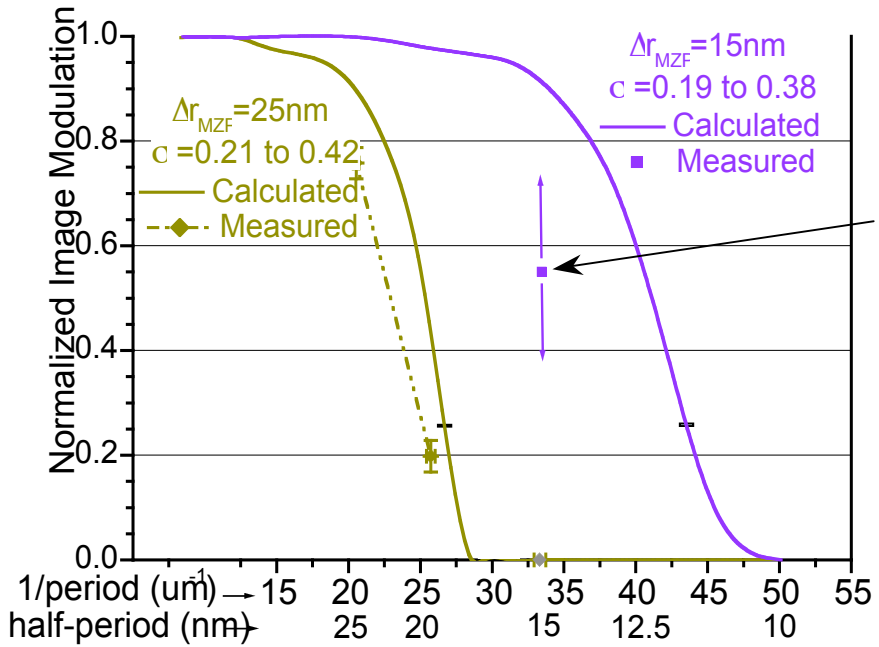

Soft x-ray image of 15 nm Cr/Si lines & spaces

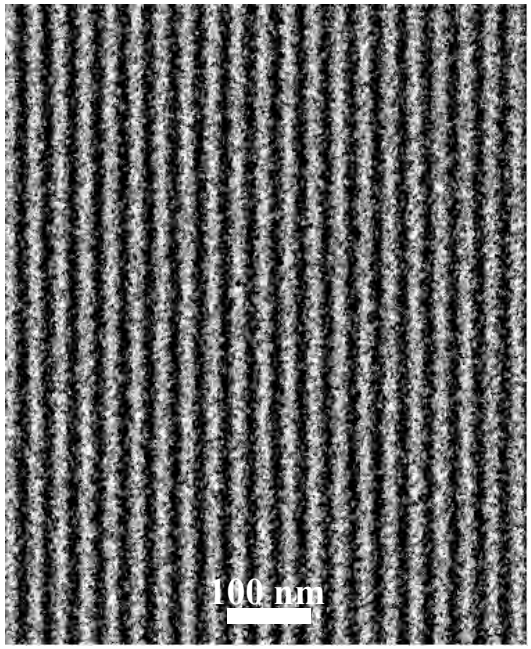

W. Chao, B. Harteneck, J.A. Liddle, E. Anderson and D. Attwood "Soft X-Ray Microscopy at a Spatial Resolution Better than 15 nm", *Nature* **435**, 1210 (30 June 2005).

Zone Plate Parameters for $\Delta r = 15$ nm, $\lambda = 2.5$ nm and $\lambda = 1.5$ nm

$\lambda = 2.5$ nm $\longrightarrow$ 1.5 nm

$\Delta r = 15$ nm

$N = 500$

$D = 30\ \mu m$

$f = 180\ \mu m \longrightarrow 300\ \mu m$

$NA = 0.083 \longrightarrow 0.05$

$$\text{Res} = \begin{cases} 18 \text{ nm } (\sigma = 0) \\ 12 \text{ nm } (\sigma = 0.4) \end{cases}$$

$\text{DOF} = \pm 180 \text{ nm} \longrightarrow \pm 300 \text{ nm}$

$\Delta\lambda/\lambda = 1/500$

Applications of Soft X-Ray Microscopy

Magnetic Recording Materials

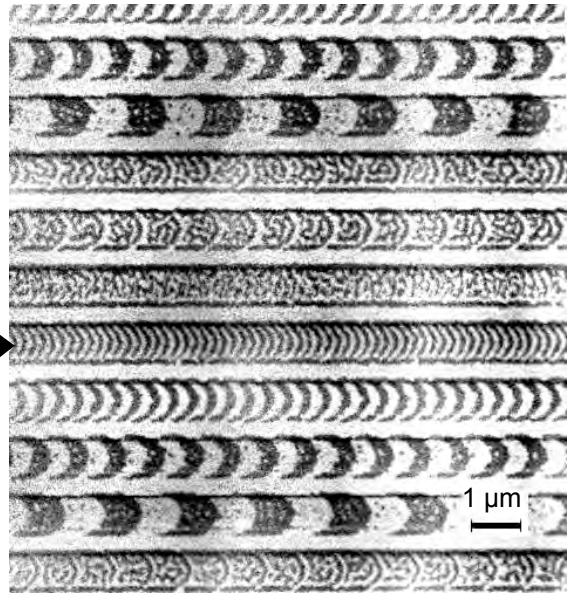

Fe L_3 @ 707.5 eV

FeTbCo Multilayer
with Al Capping Layer

Courtesy of P. Fischer (Max Planck)
and G. Denbeaux (CXRO/LBNL)

Cryo Microscopy for the Life Sciences

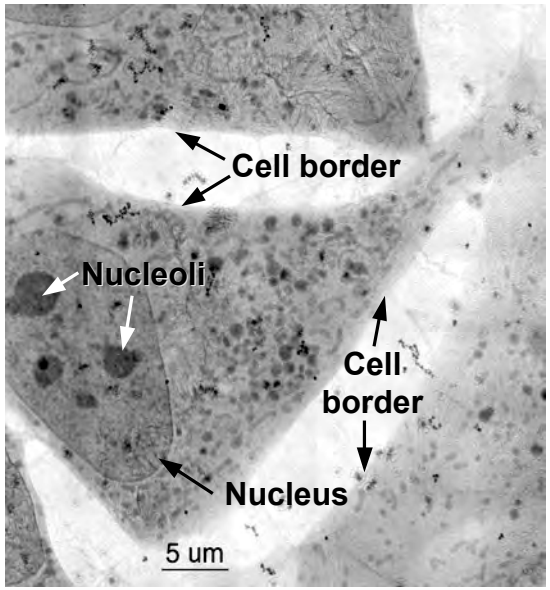

Cryo X-Ray Microscopy
of 3T3 Fibroblast Cells

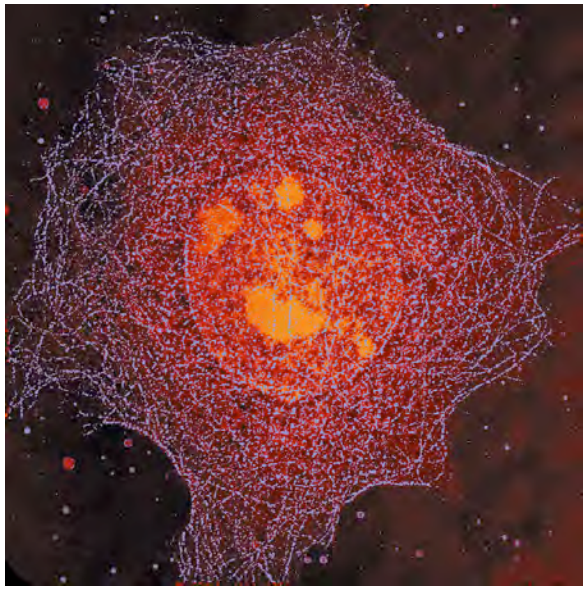

Protein Labeled
Microtubule Network

Courtesy of C. Larabell (UCSF)
and W. Meyer-Ilse (CXRO/LBNL)

The Water Window for Biological X-Ray Microscopy

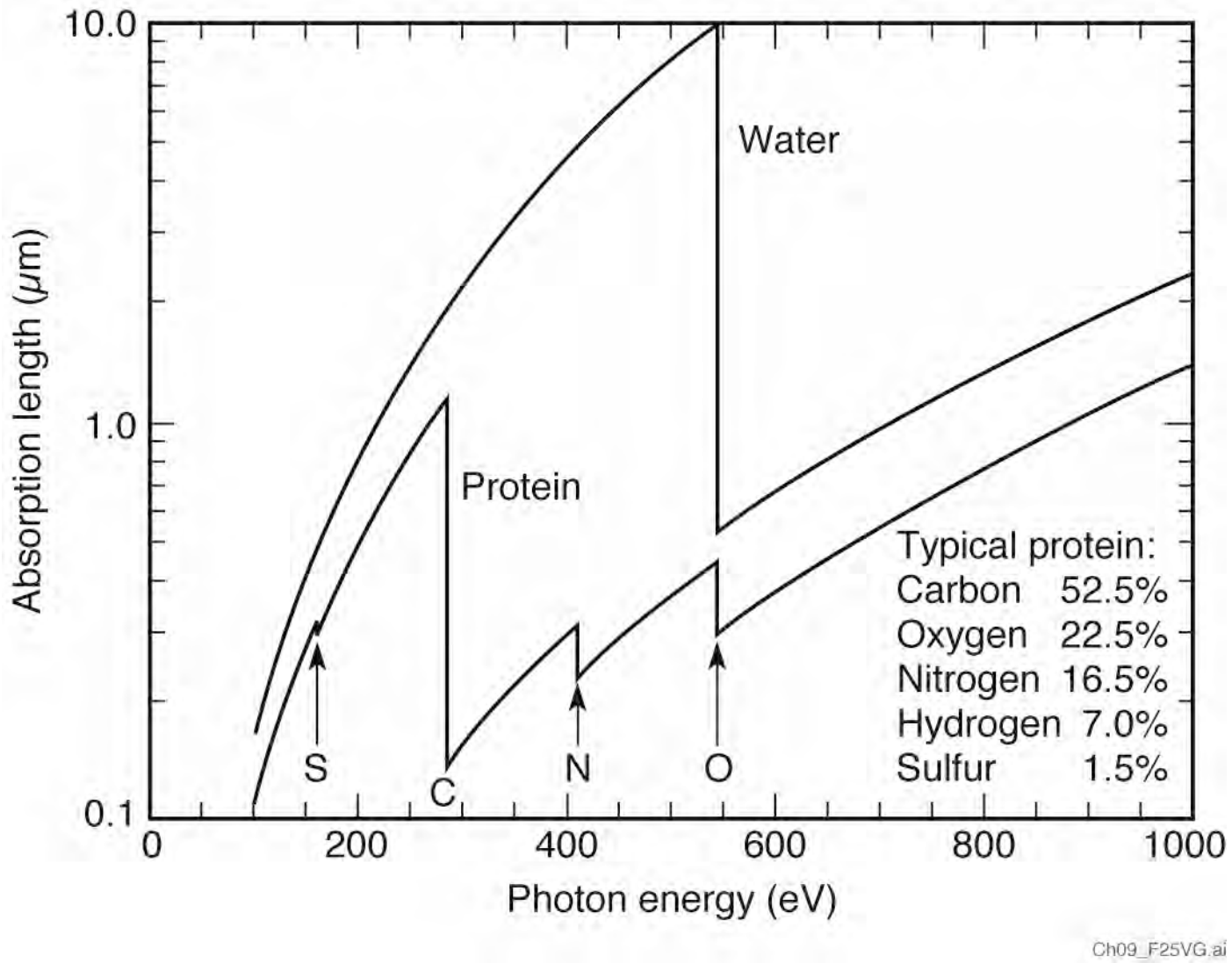

Fast Freeze Cryo Fixation Strongly Mitigates Radiation Dose Effects

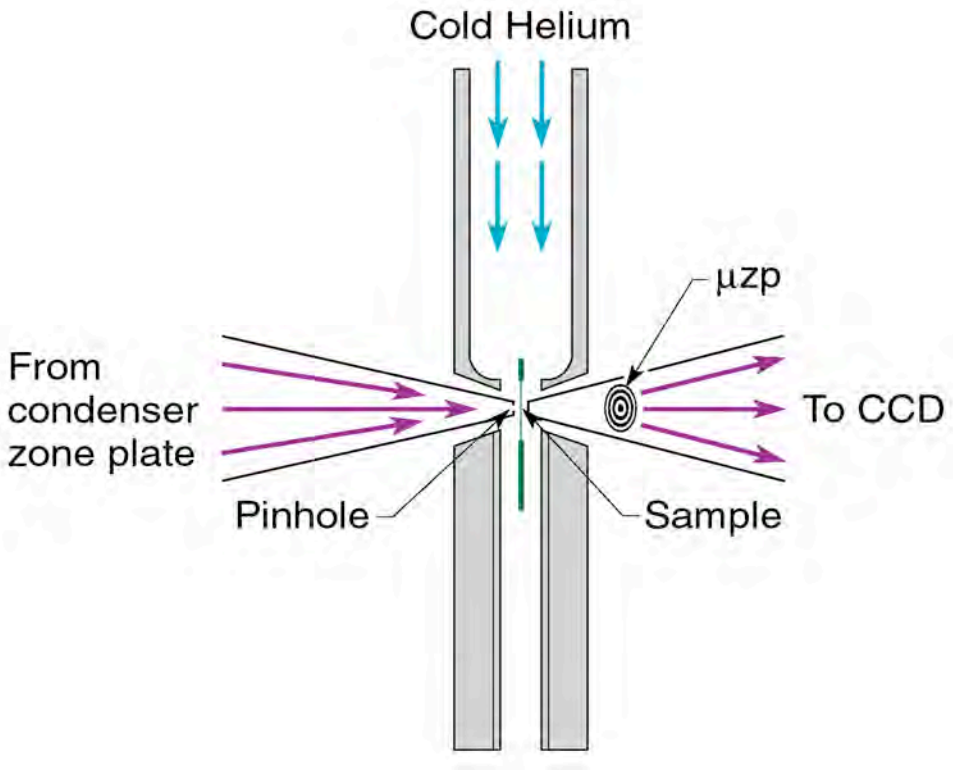

Helium passes through LN, is cooled, and directed onto sample windows

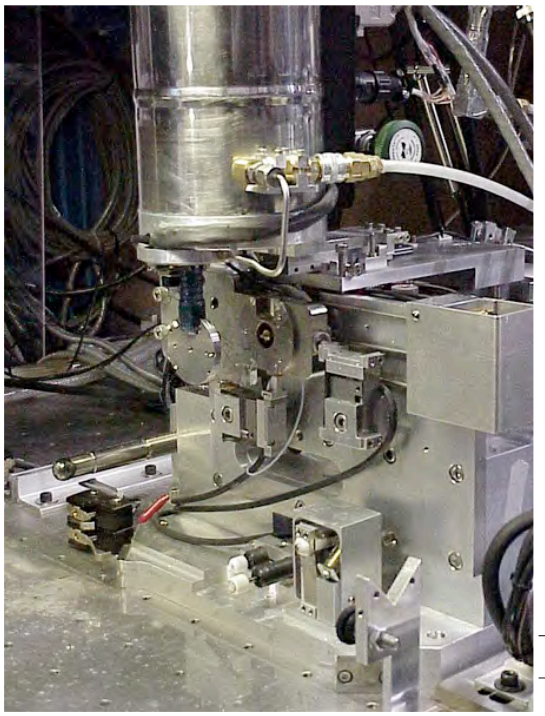

Fast Freeze

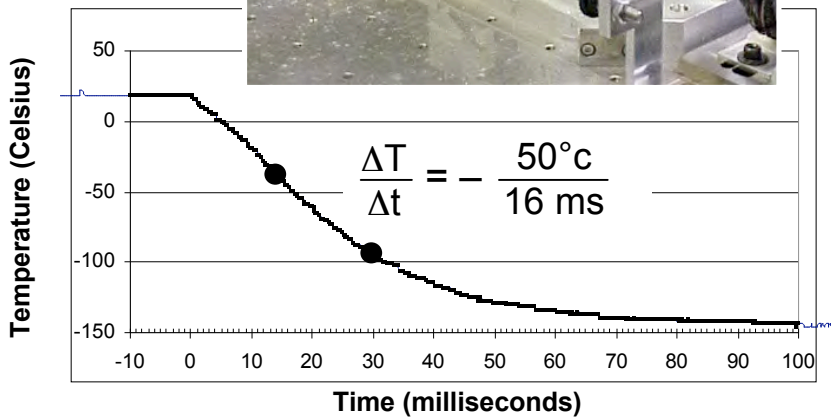

W. Meyer-Ilse, G. Denbeaux, L. Johnson, A. Pearson (CXRO-LBNL)

Organelle Details Imaged with Cryogenic Preservation and High Spatial Resolution

Cryo x-ray microscopy of 3T3 fibroblast cells

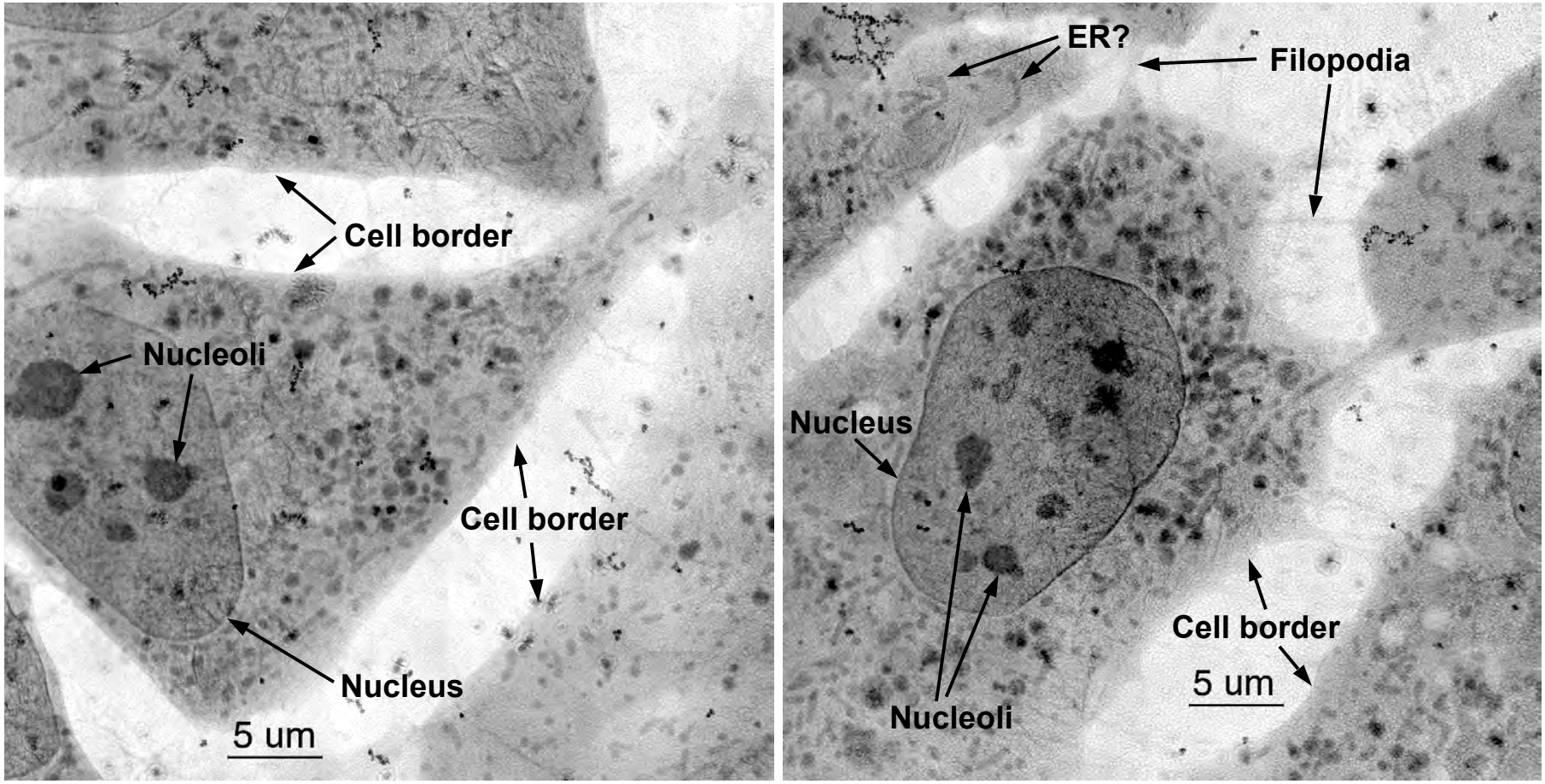

C. Larabell, D. Yager, D. Hamamoto, M. Bissell, T. Shin (LBNL Life Sciences Division)
W. Meyer-Ilse, G. Denbeaux, L. Johnson, A. Pearson (CXRO-LBNL)

Bending Magnet Radiation Used With a Soft X-Ray Microscope to Form a High Resolution Image of a Whole, Hydrated Mouse Epithelial Cell

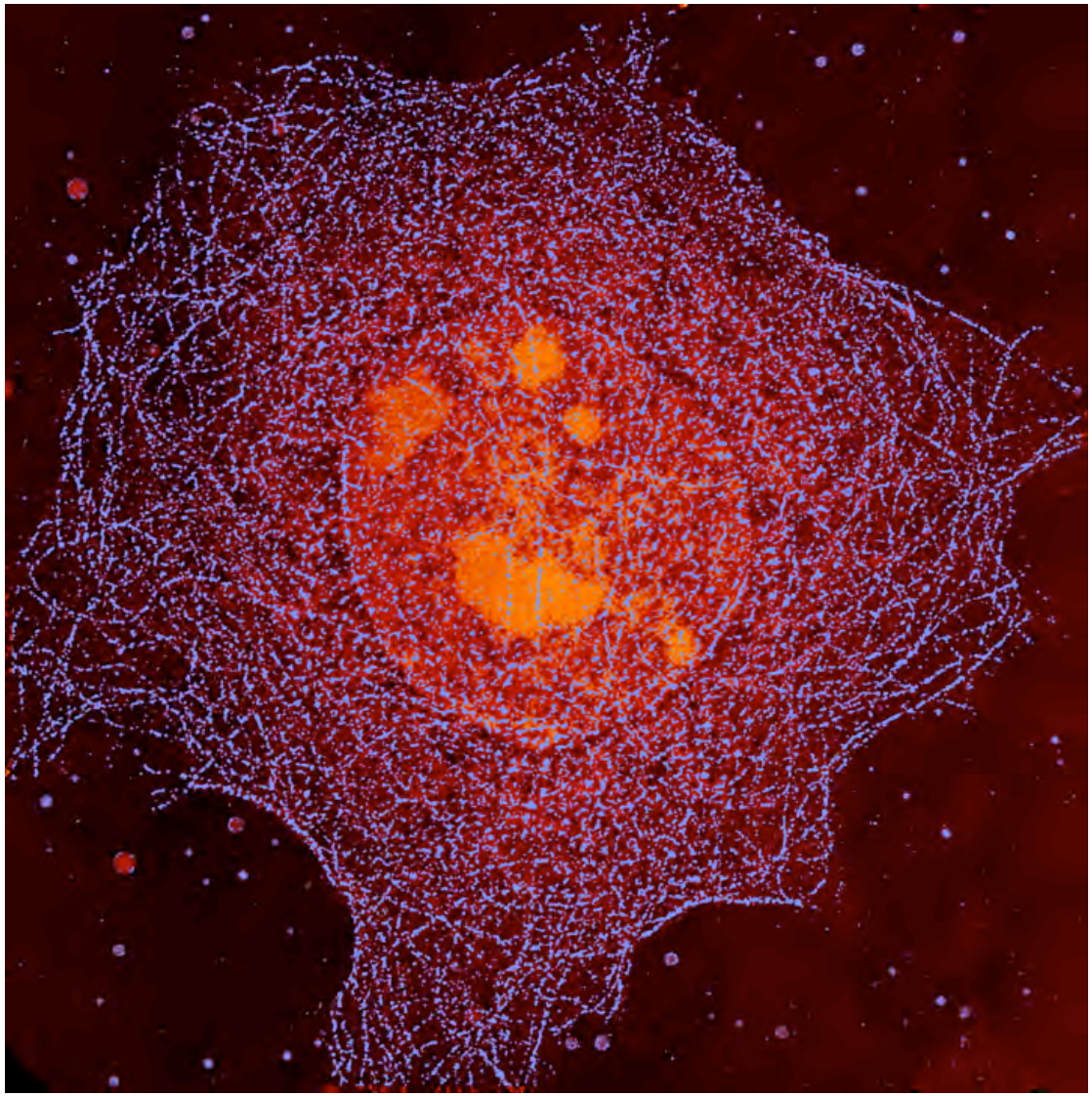

$\hbar w$ = 520 eV

32 μm x 32 μm

Ag enhanced Au labeling of the microtubule network, color coded blue.

Cell nucleus and nucleoli, moderately absorbing, coded orange.

Less absorbing aqueous regions coded black.

W. Meyer-Ilse et al.
J. Microsc. 201, 395 (2001)

Courtesy of C. Larabell and W. Meyer-Ilse (LBNL)

NCXT National Center for X-ray Tomography
An NIH/DOE Biomedical Technology Resource

XM-2: A New, Upgraded Microscope Dedicated to Soft X-Ray Biotomography

BERKELEY LAB

- Dedicated to life sciences research
- Cryotomography without apparatus interruption
- Interchangeable objective lenses (tradeoff resolution, depth of focus, working distance)
- Improved resolution, lens efficiency, image contrast and uniformity
- Improved cryo transport
- Improved computational image reconstruction and analysis
- More flexible use of phase contrast

Magnetic X-Ray Microscopy Using X-Ray Magnetic Circular Dichroism (XMCD)

Magnetic X-Ray Microscopy

- High spatial resolution in transmission
- Bulk sensitive (thin films)
- Complements surface sensitive PEEM
- Good elemental sensitivity
- Good spin-orbit sensitivity
- Allows applied magnetic field
- Insensitive to capping layers
- In-plane and out-of-plane measurements

Courtesy of P. Fischer, Wuerzberg and G.Denbeaux, CXRO/LBNL

Imaging of Thermomagnetically Written Bits in MO Media

100 nm lines & spaces →

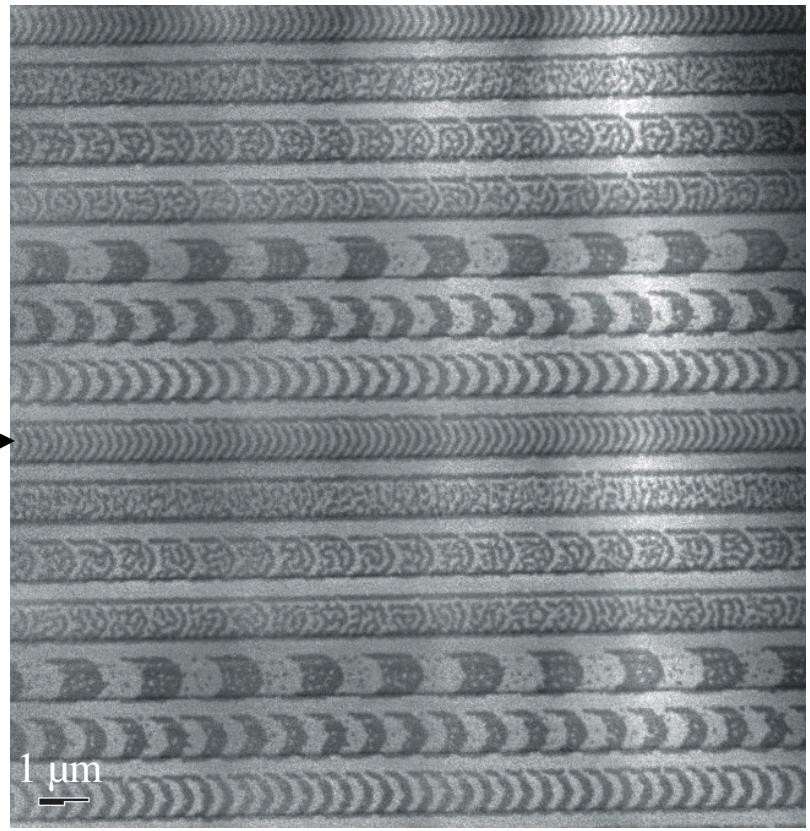

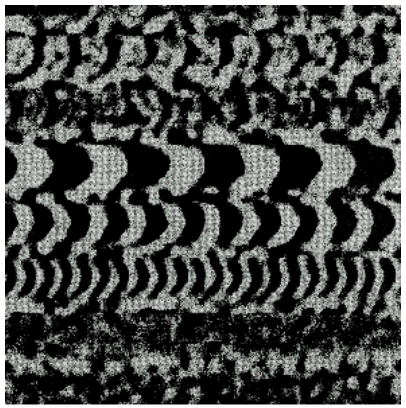

MFM-image

$SiN(70\ nm)/Tb_{25}(Fe_{75}Co_{25})_{75}(50\ nm)/SiN(20\ nm)/Al(30\ nm)/SiN(20\ nm)$

P. Fischer et al., Wuerzburg; N. Takagi et al., Sanyo; G. Denbeaux et al., CXRO/LBNL

Magnetic Domains Imaged at Different Photons Energies

FeGd Multilayer

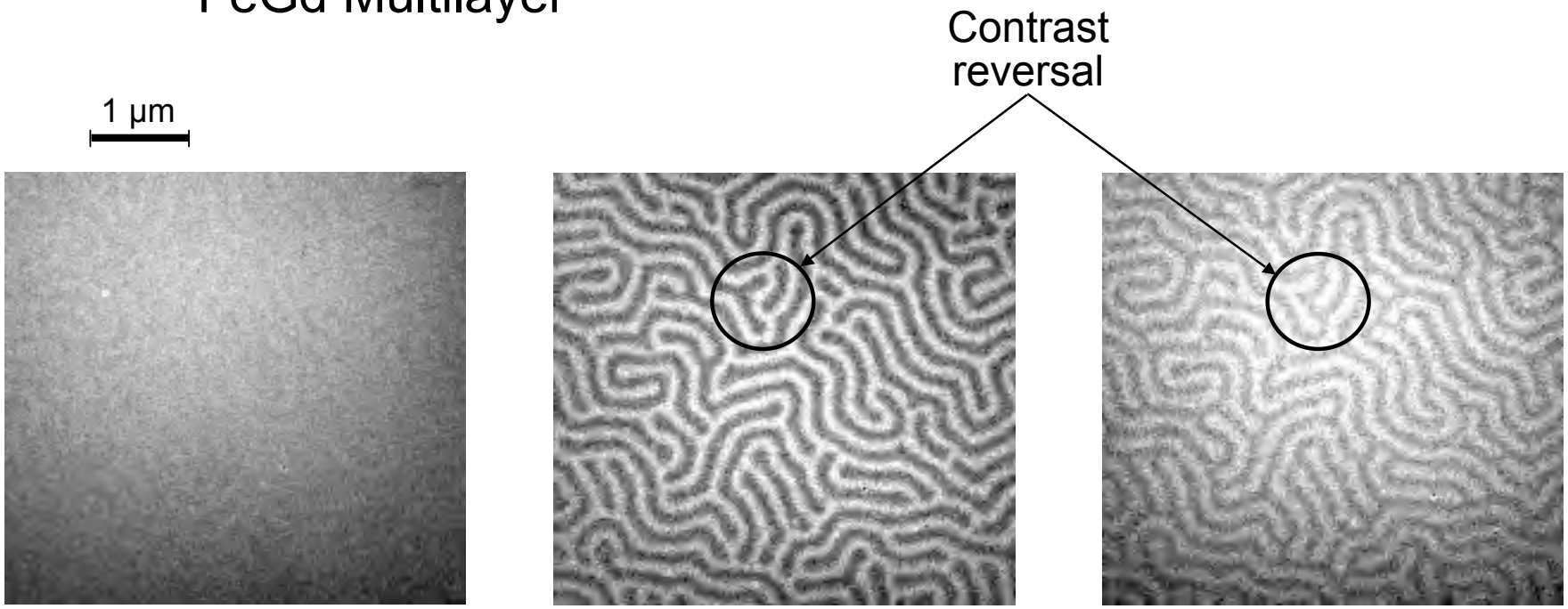

ħω = 704 eV
below Fe L-edges

ħω = 707.5 eV
Fe L_3-edge

ħω = 720.5 eV
Fe L_2-edge

P. Fischer, T. Eimueller, M. Koehler (U. Wuerzberg)
S. Tsunashima (U. Nagoya) and N. Tagaki (Sanyo)
G. Denbeaux, L. Johnson, A. Pearson (CXRO-LBNL)

Nanoscale Local Hysteresis

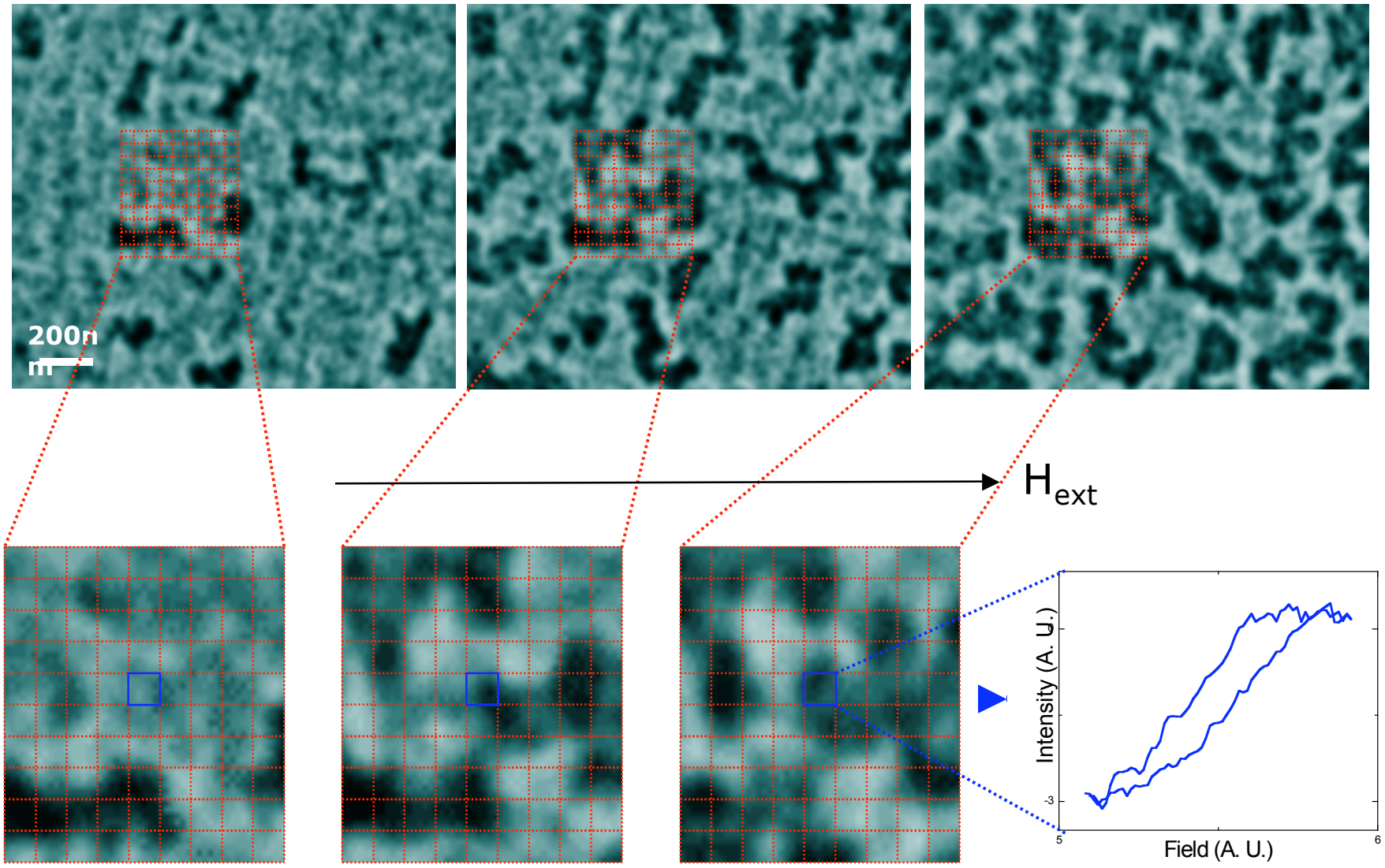

D.-H. Kim et al., J. Appl. Phys. (2005) accepted

Electromigration in Latest Technology Computer Chips with Cu vias Connecting Multilevel Metallization Layers

SEM micrograph

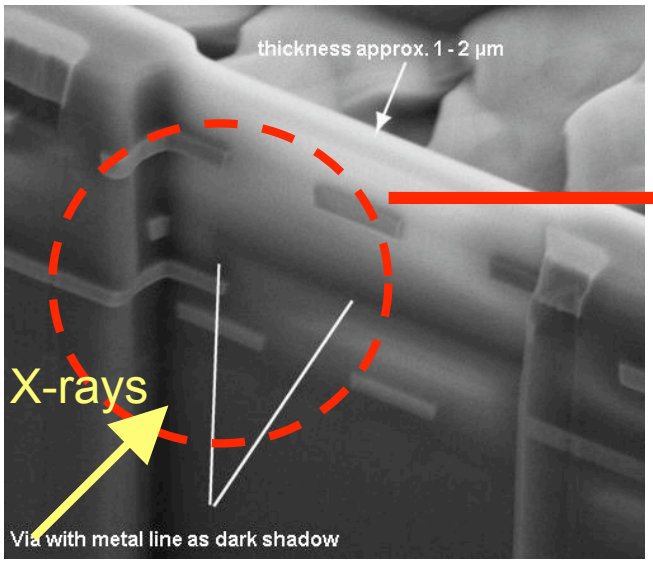

X-ray micrograph imaged at 1.8 keV

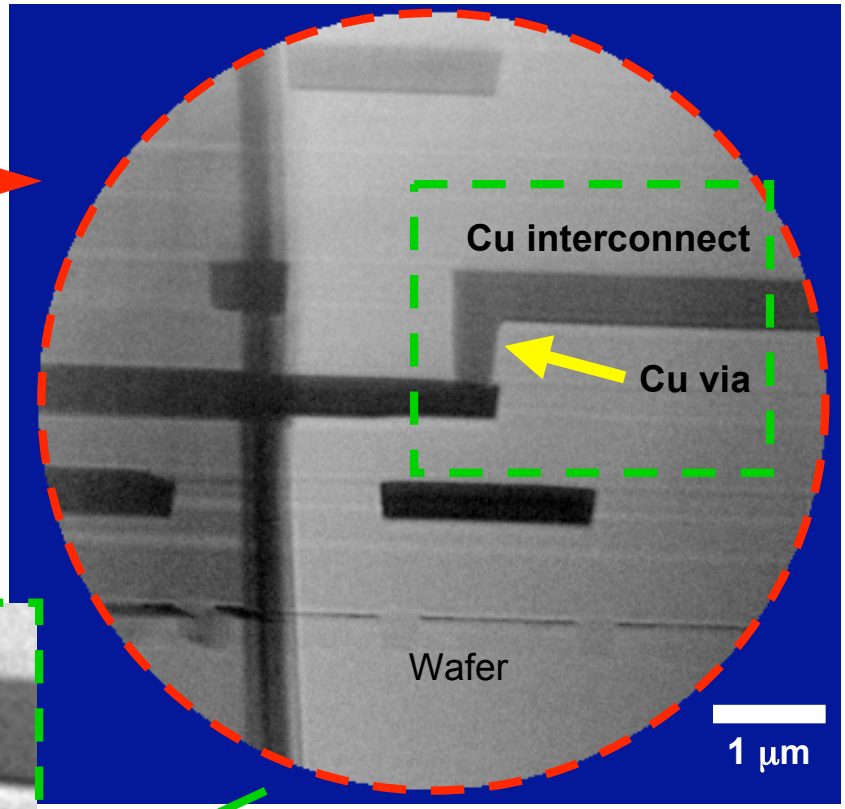

TXM (1.8 keV photons)

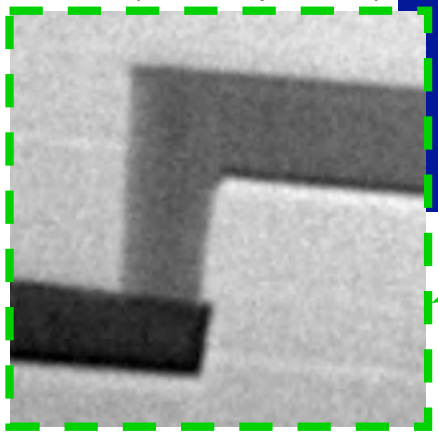

HVTEM (0.8 MeV electrons)

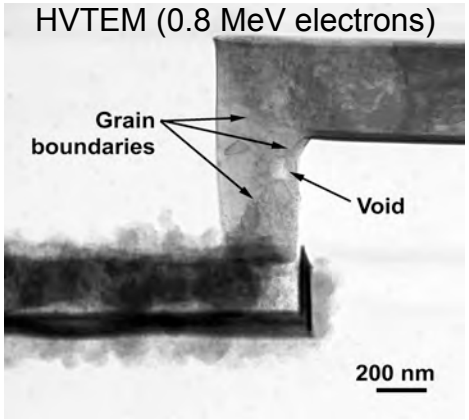

High current density

Courtesy of Gerd Schneider (BESSY)

G. Denbeaux, E. Anderson, A. Pearson and B. Bates (CXRO)
M. Meyer and E. Zschech (AMD Saxony Manufacturing GmbH) / E. Stach (NCEM / LBNL)

Using Phase Effects to Achieve Higher Diffraction Efficiency

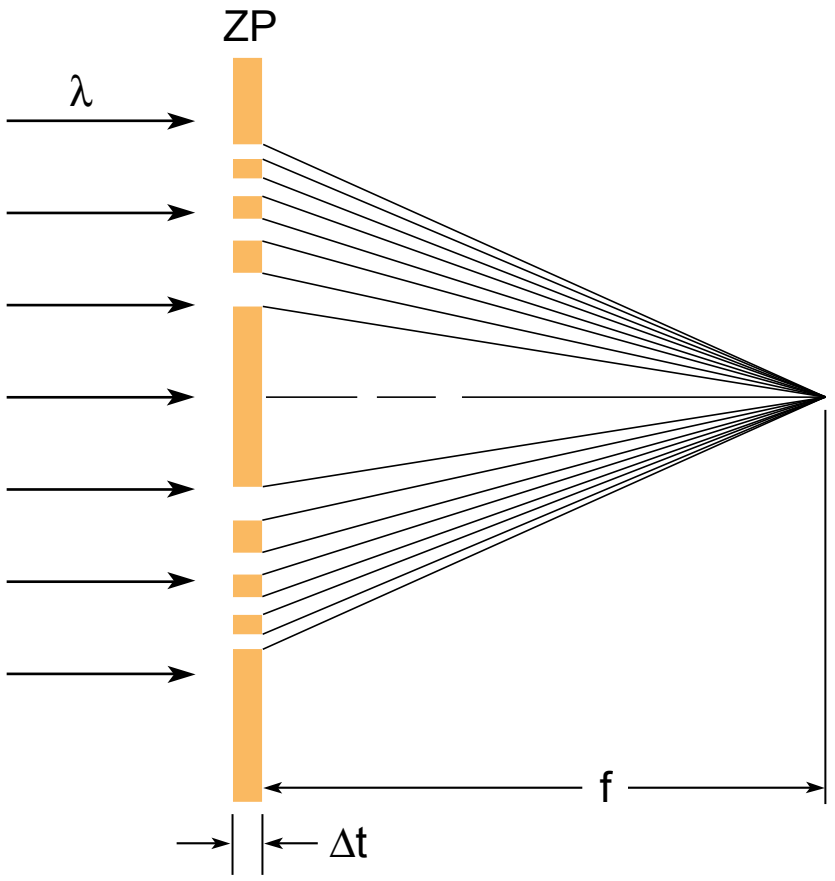

$$\Delta\phi = \left(\frac{2\pi\delta}{\lambda}\right)\Delta t \qquad (3.29)$$

For a π-phase shift

$$\Delta t = \frac{\lambda}{2\delta} \qquad (9.25)$$

a factor of four can be gained in diffraction efficiency. For soft x-rays and EUV all materials are partially absorbing

$$n = 1 - \delta + i\beta \qquad (3.12)$$

Optimization is a function of δ/β, as discussed by J. Kirz, J. Opt. Soc. Am. 64, 301 (1974) and by G.R. Morrison, Ch. 8 in A. Michette and C. Buckley, X-Ray Science and Technology (IOP, Bristol, 1993).

Hard X-Ray Zone Plate Microscopy

Images courtesy of the Synchrotron Radiation Research Center (SRRC), Taiwan

Gung-Chian Yin

Mau-Tsu Tang

and Xradia, Concord, CA

Wenbing Yun

Michael Feser

The Transmission X-ray Microscope

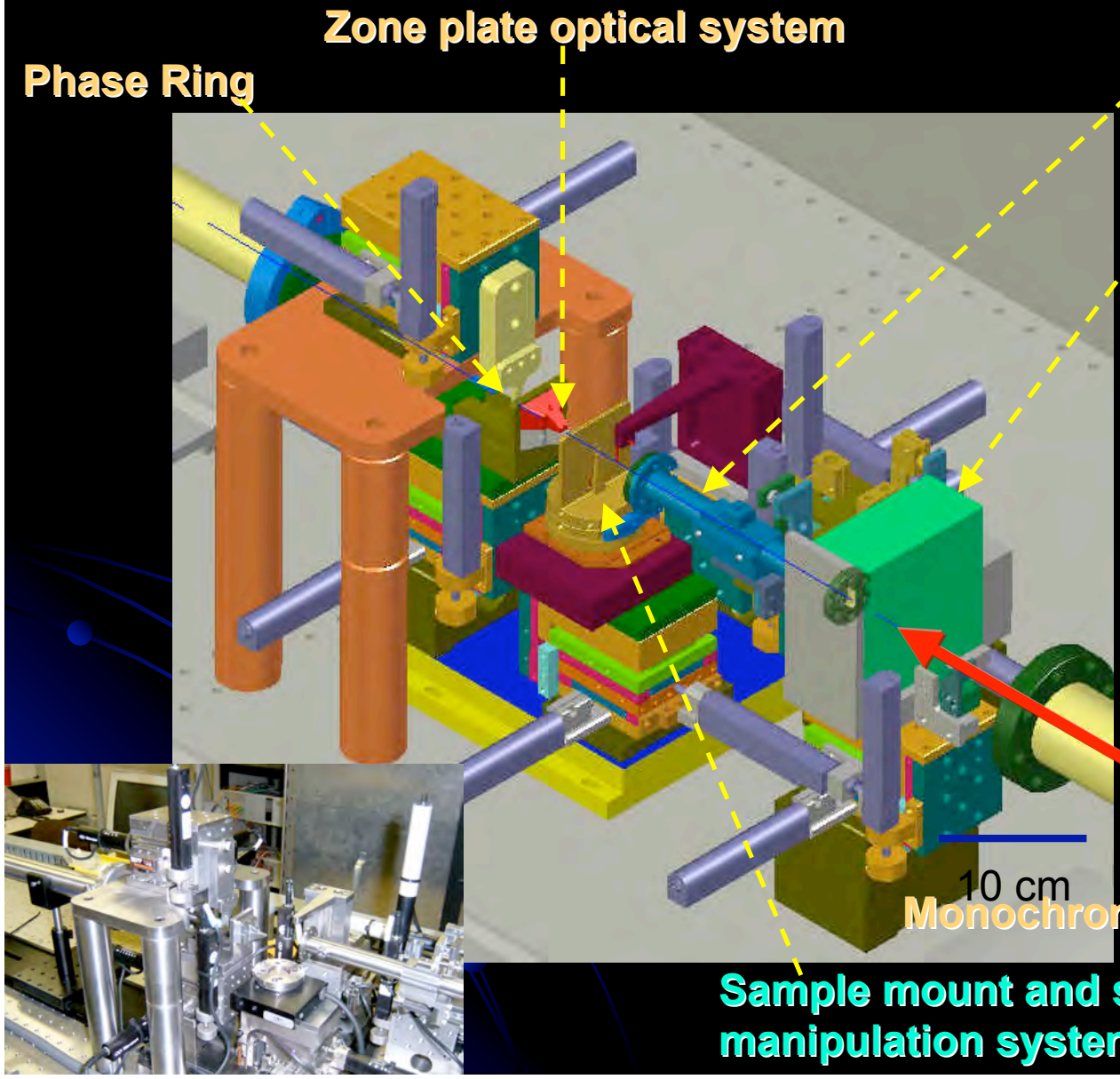

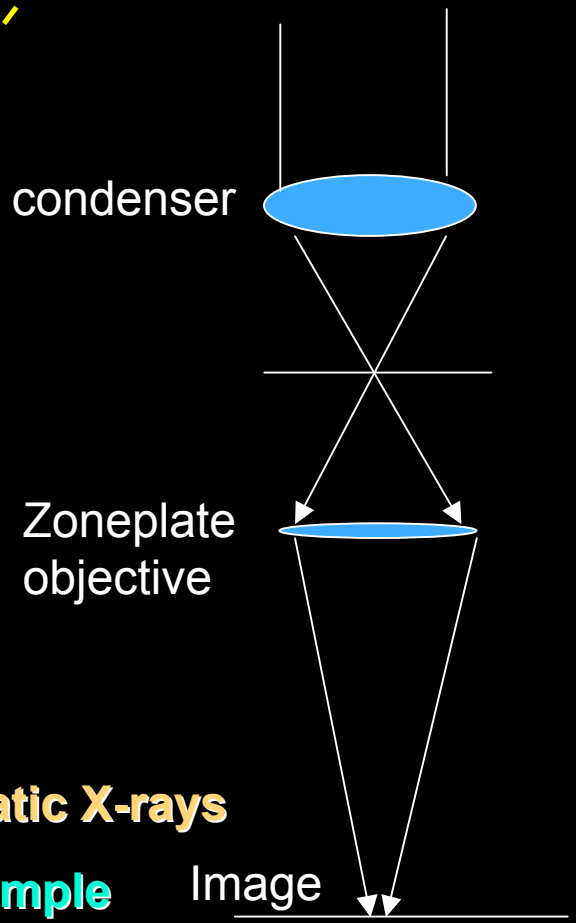

The resolution reaches 30 nm.

APL v89,221122,2006

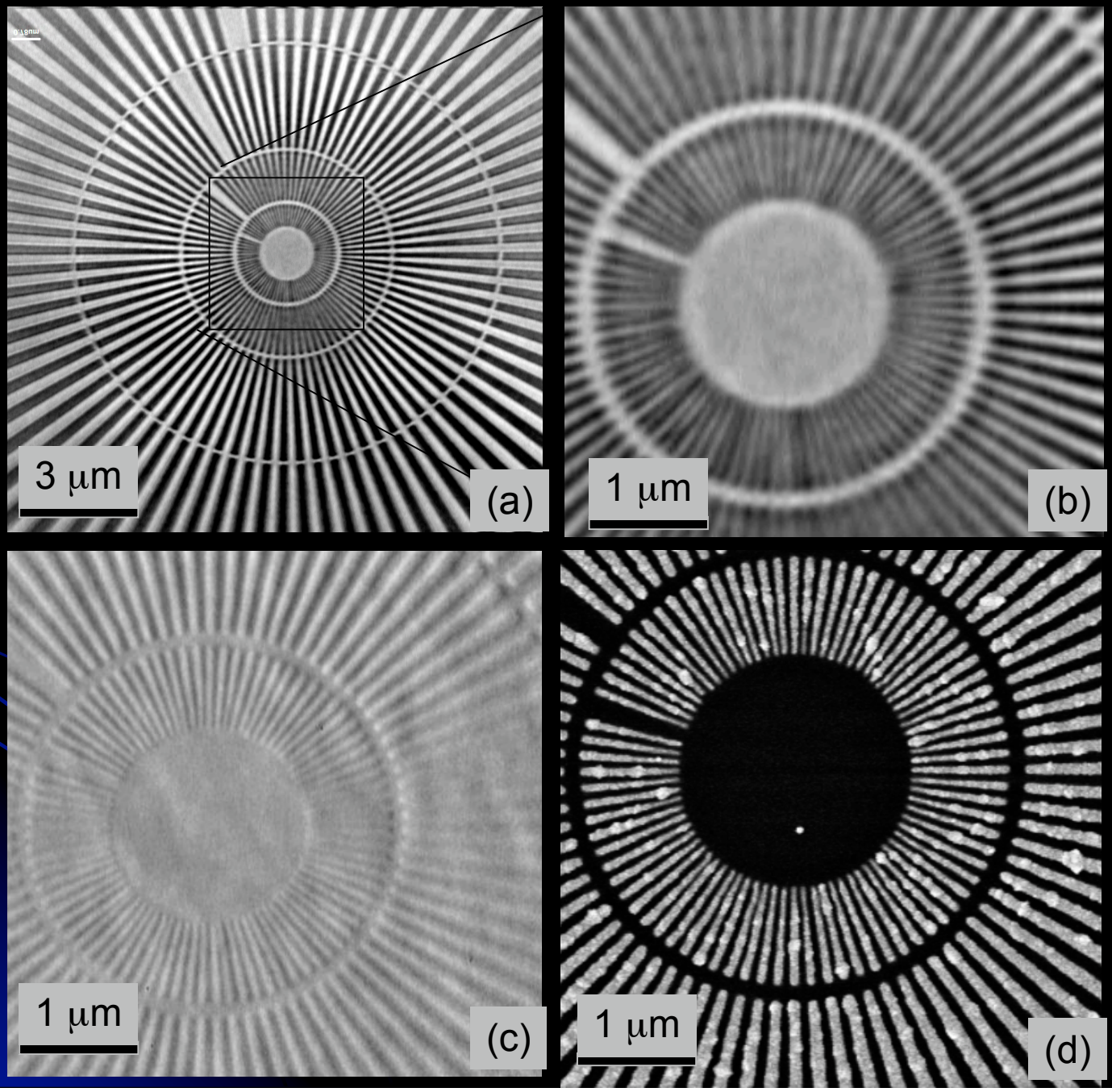

TXM with Zernike's phase contrast method

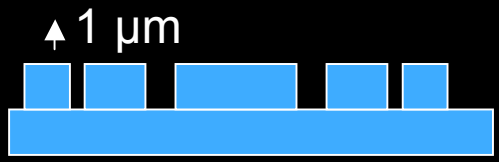

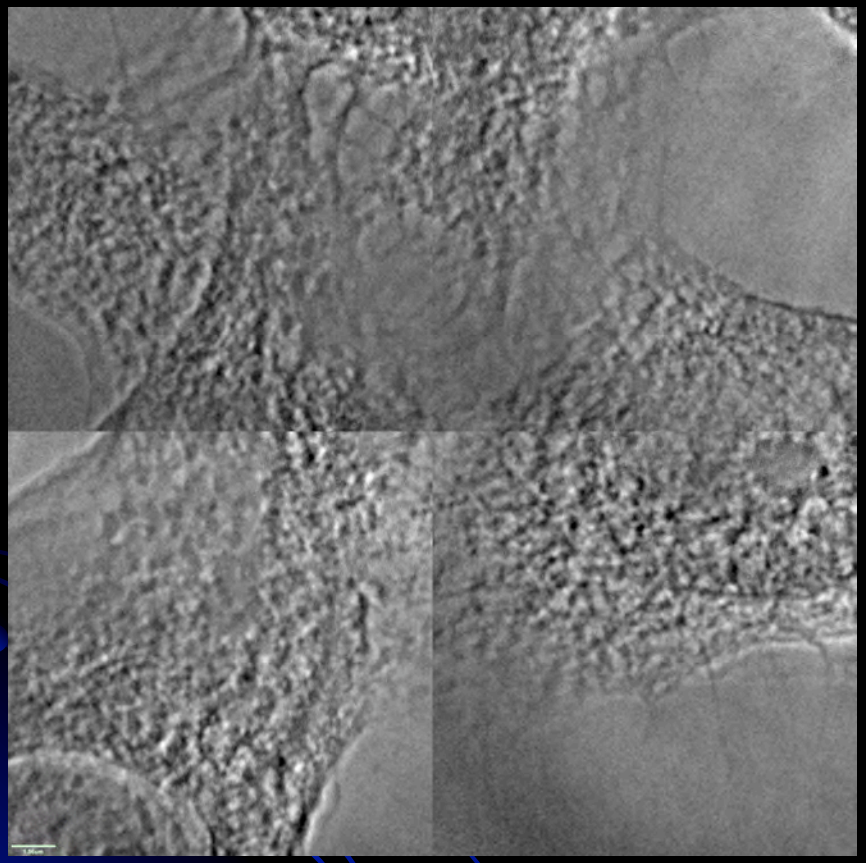

HeLa cell with Nicole stained

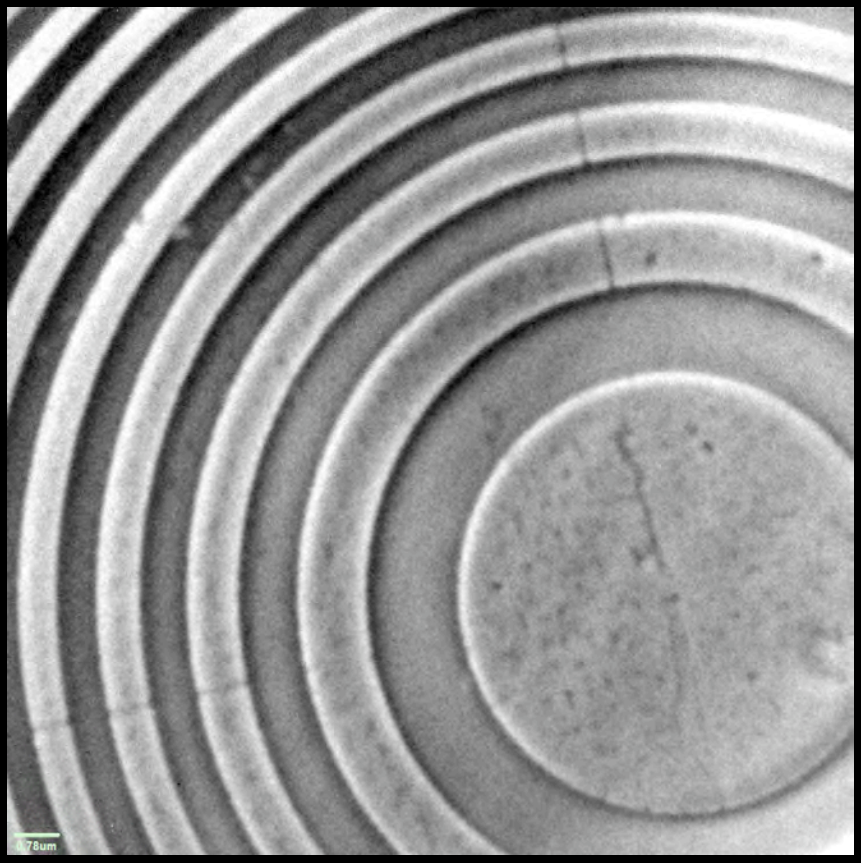

Plastic zoneplate of 1 μm thick

The tomography close 60 nm.

APL. Vol 88, 241115,2006

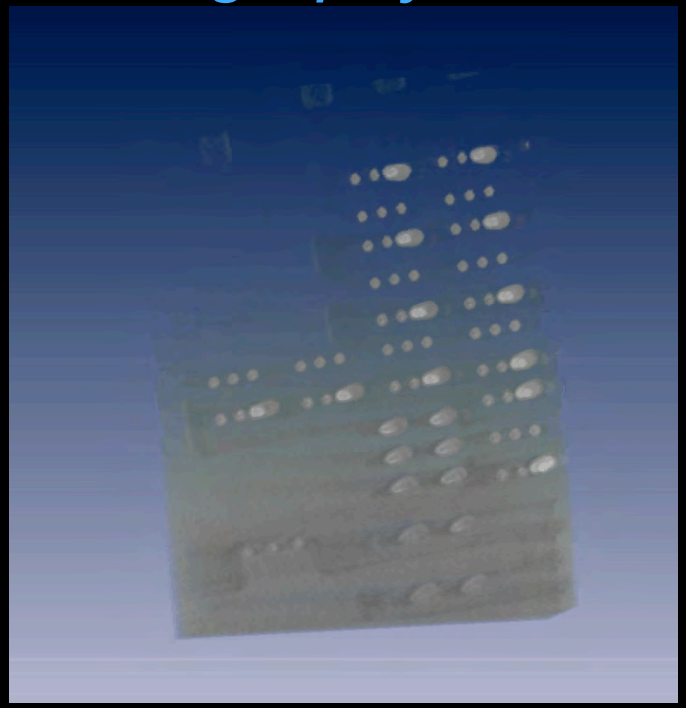

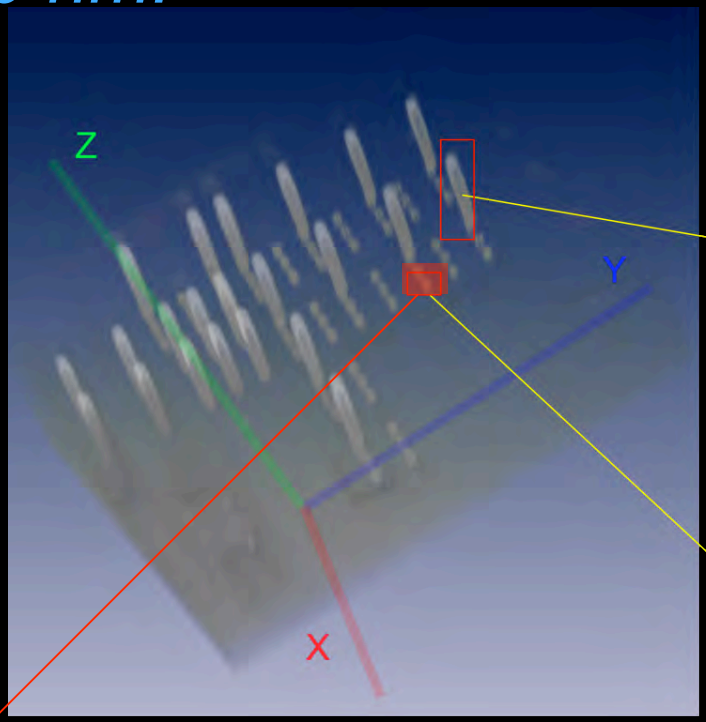

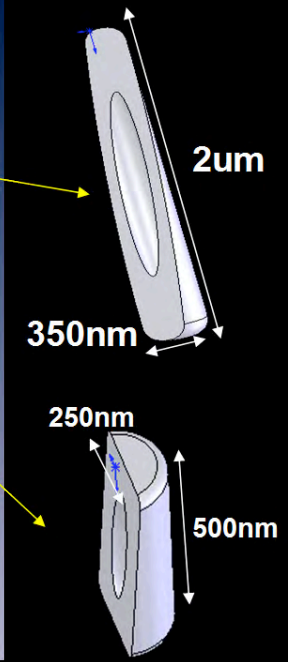

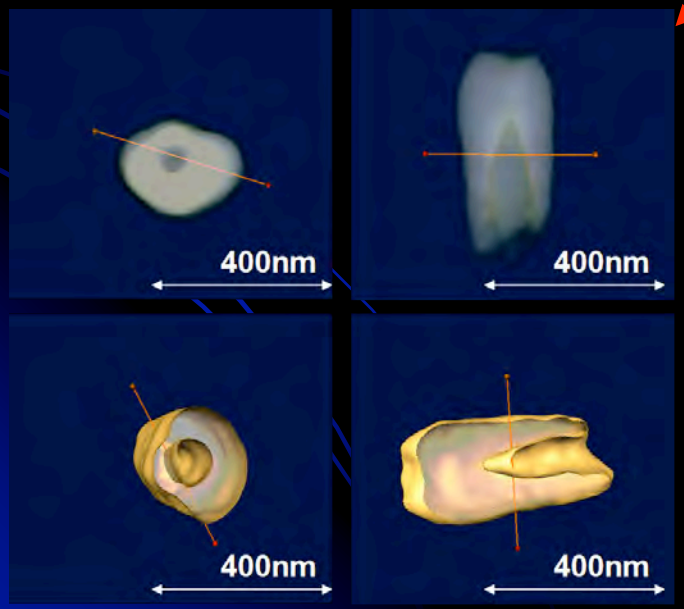

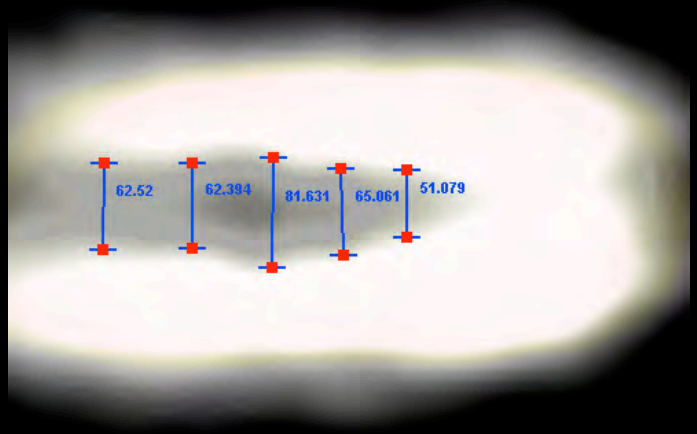

MICROSCOPY

Nanotomography comes of age

David Attwood

The use of X-rays to construct three-dimensional tomographic images is well established in medicine. The same principle is being extended to the nanoscale, bringing us startlingly accurate pictures of tiny objects.

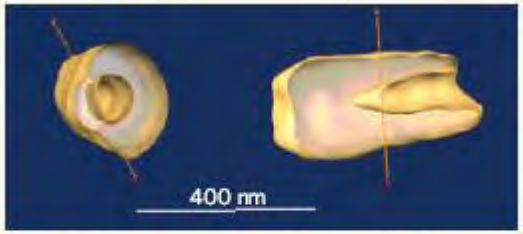

Figure 1 | Plug away. Yin *et al.*[1] use data from 141 two-dimensional X-ray images obtained at 1° angular increments to construct a three-dimensional data set of tungsten plugs used as electrical interconnects between layers of a computer chip. By imaging at an X-ray photon energy of 10.5 keV, just above a tungsten absorption edge, a void of 50–80 nm diameter is clearly seen in the roughly 250 × 500-nm tungsten plugs. (Courtesy of G.-C. Yin.)

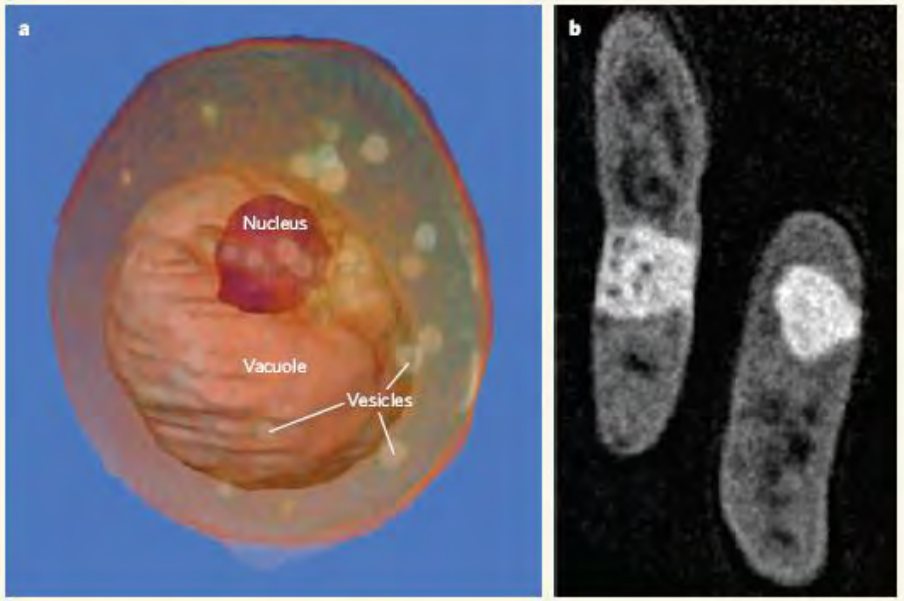

Figure 2 | Nanoscale bio-tomography. **a**, Tomographically reconstructed image of a whole, hydrated yeast cell about 5 μm wide, based on 45 two-dimensional images obtained at 4° angular increments, covering 180°. At the incident photon energy of 517 eV, water is relatively transparent and carbon absorbs, providing a natural contrast mechanism. The cell nucleus, a large vacuole and several lipid-filled vesicles are visible. **b**, Tomographic software can be used to produce images through various planes in an object. Here, a computer-generated section through two *Escherichia coli* bacteria, each about 0.5 μm wide, were obtained from a similar three-dimensional data set from 45 images at 4° intervals and 2.4 nm wavelength. The nature of the large white bands and dark sub-structure is unknown. Typical exposure times are 1–3 seconds per two-dimensional image; it takes about 5 minutes for acquisition of a full data set. (Courtesy of C. Larabell, UCSF and LBNL[4,5].)

Nature: Aug 2006

Application: Advanced IC Device

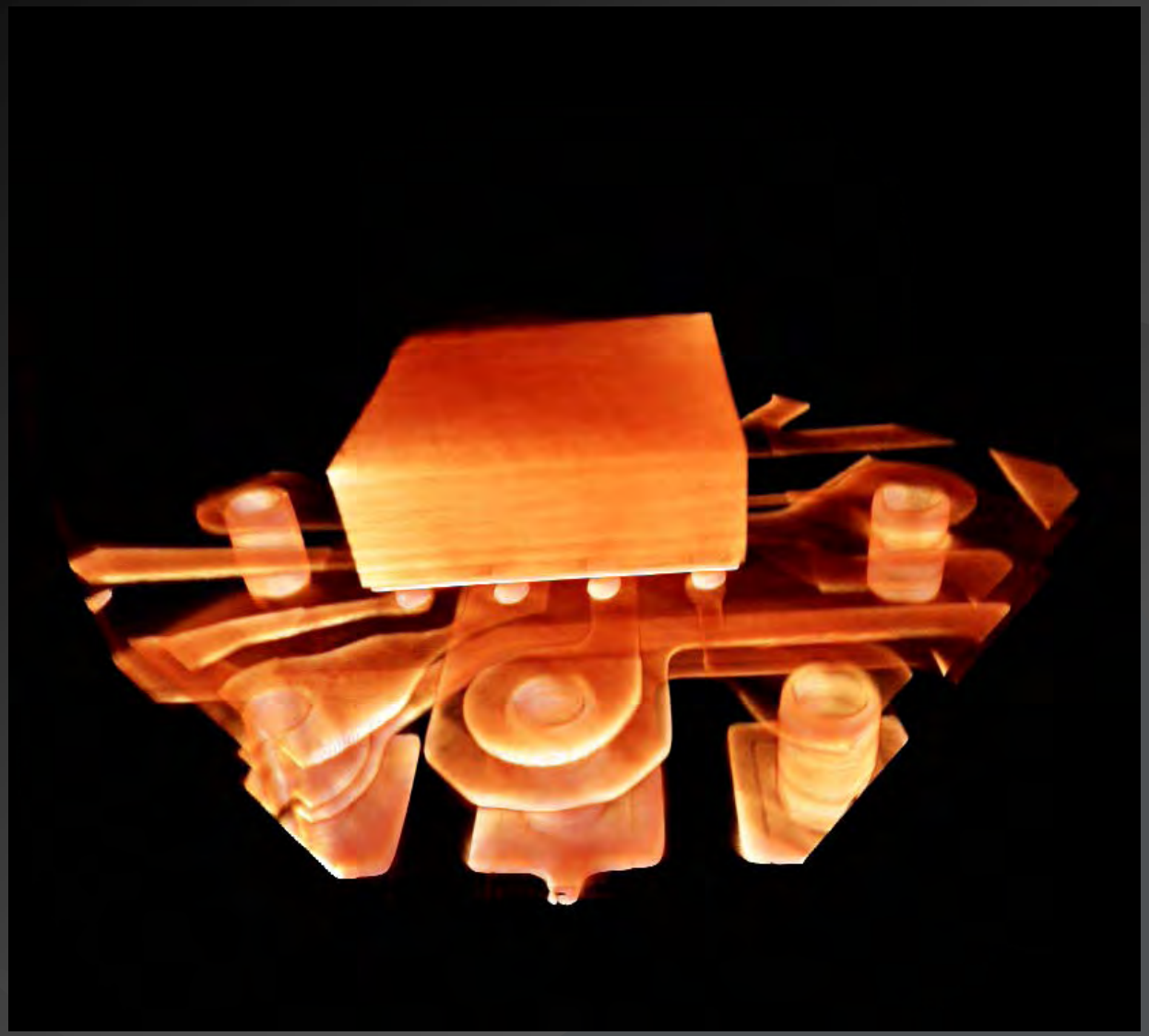

Failure analysis and R&D of advanced IC devices

nanoXCT: Schematic and Challenges

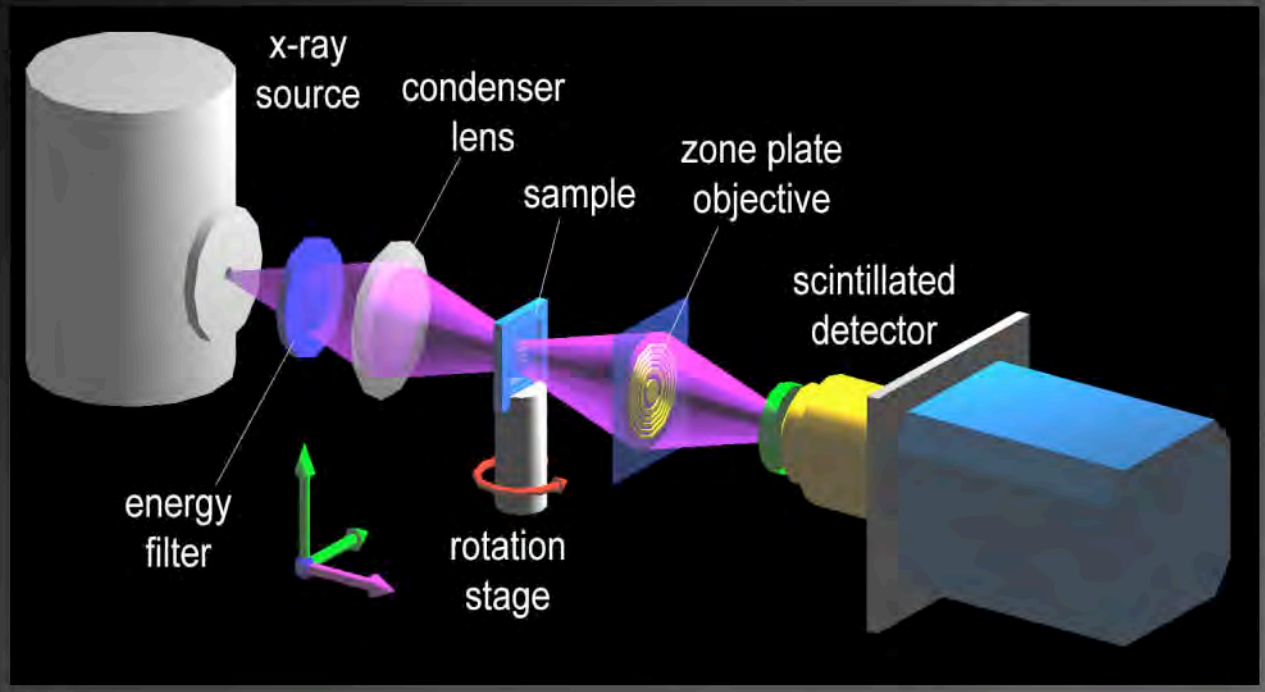

X-ray Zone-plate Lens

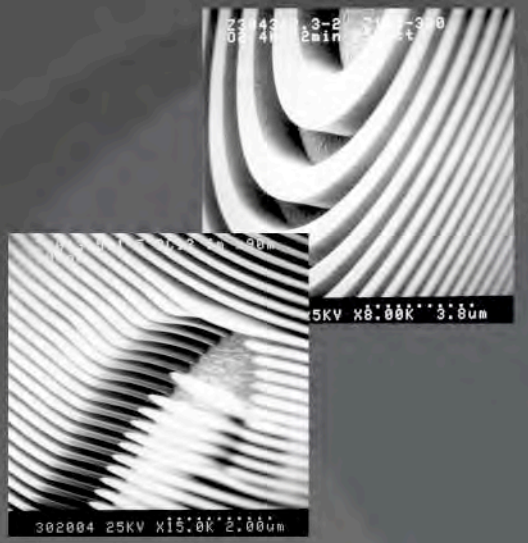

Challenges for achieving nm scale resolution:

- High resolution objective lens: limiting the ultimate resolution
- High numerical aperture condenser lens:
- Detector: high efficiency for lab. source and high speed for synchrotron sources
- Precision mechanical system

nanoXCT 8-50-S: Sub-25 nm Hard X-ray Image

Xradia Resolution Pattern
X-50-30-1

- 50 nm bar width
- 150 nm thick Au

- 8keV x-ray energy

F. Duewer, M. Tang,
G. C. Yin, W. Yun, et al.

Xradia nano-XCT 8-50S
installed at NSRRC,
Taiwan
3rd diffraction order image

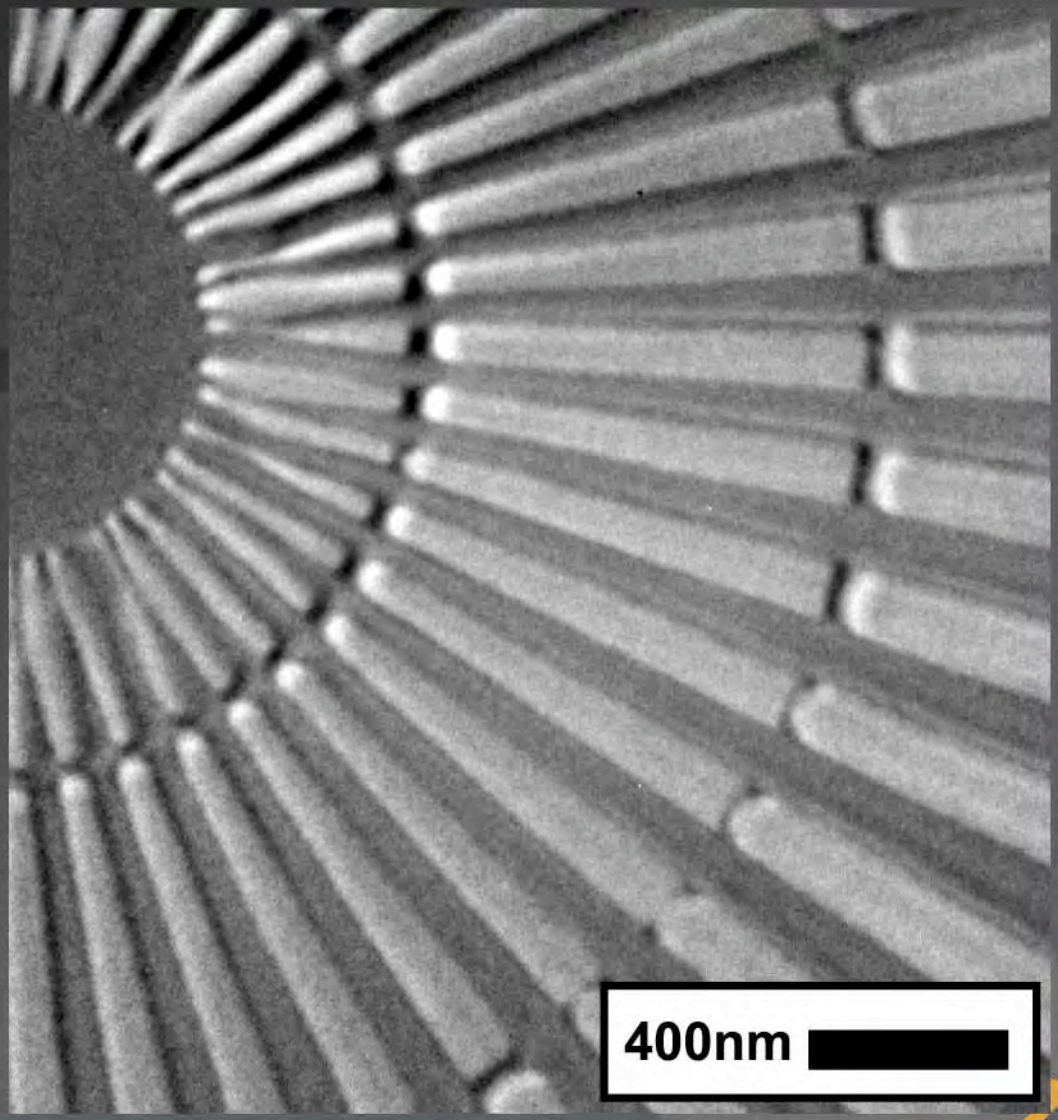

Phase Contrast: Composite Polymer

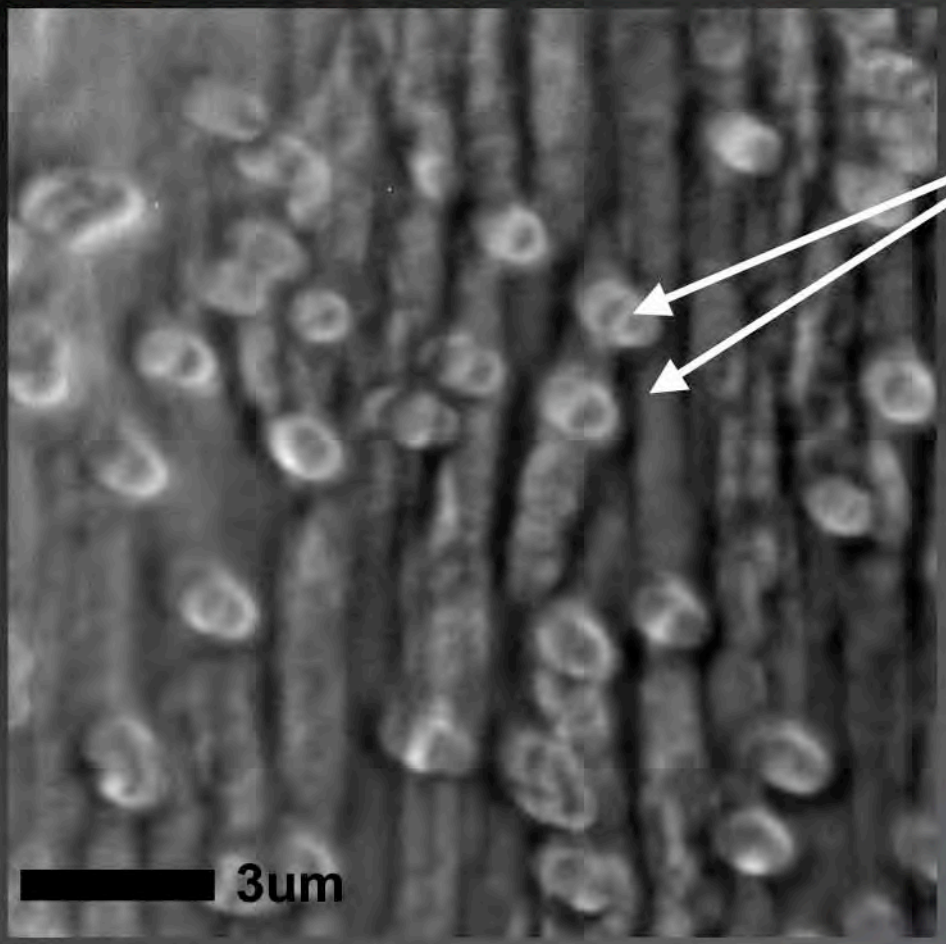

G. C. Yin, et al.
Xradia nanoXCT S-60
NSRRC - Taiwan

- Ability to image small density differences of different polymer compositions
- Ability to image polymer alloy phase structure, fiber alignment, additive distribution
- Not possible to image with absorption contrast

- ***4 sec exposure*** @8kV (Synchrotron)

Elemental Contrast by Tuning Energy across Specific Absorption Edge (Guan-Chian Yin *et al*)

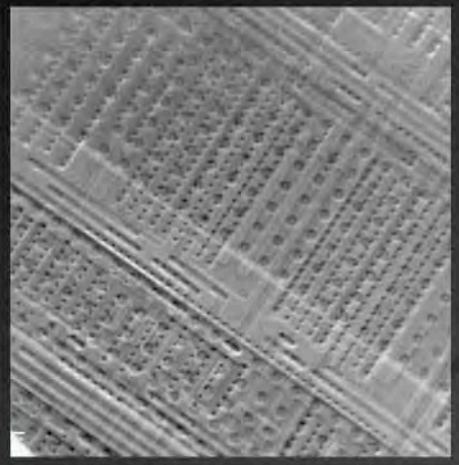

8.4 keV

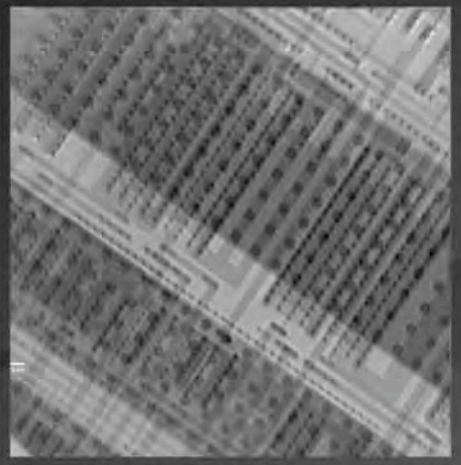

9.5 keV

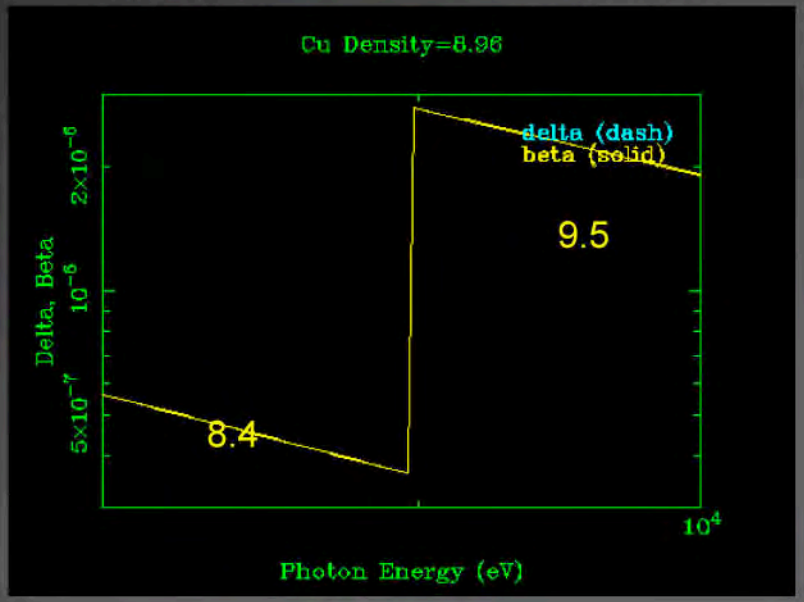

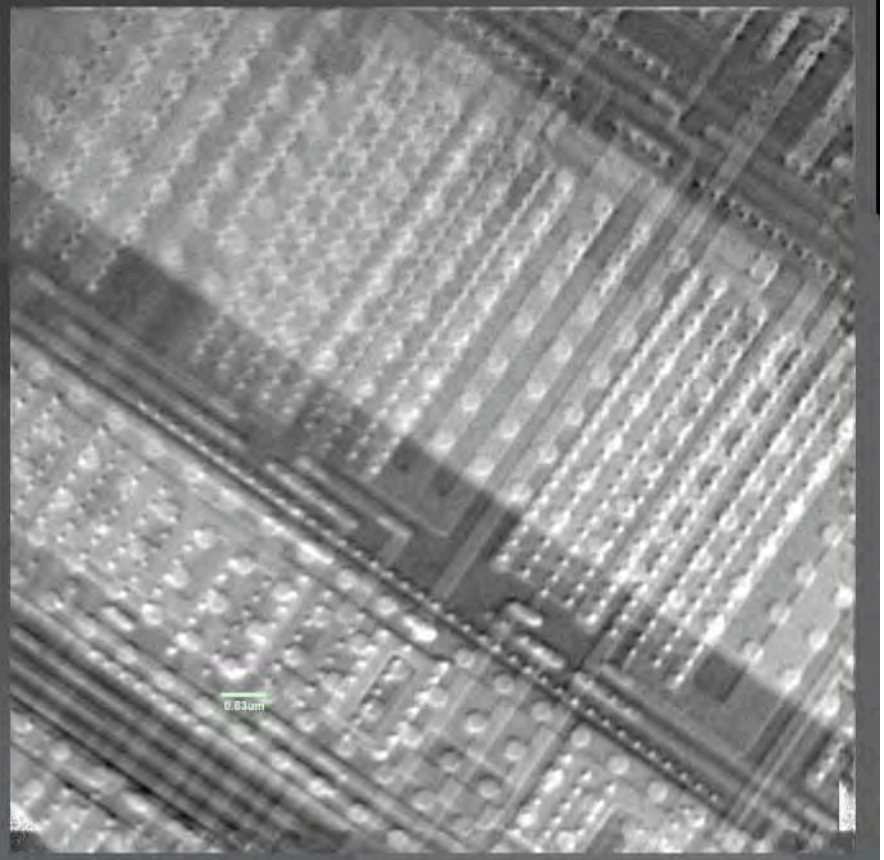

Intensity difference between
E = 8.4 keV and 9.5 keV

SSRL nanoXCT installation

- Installed Dec 2006 in 1 day
- 1s exposure time at 8keV Zernike phase contrast
- <30nm resolution in first order imaging mode

The Scanning Soft X-Ray Microscope

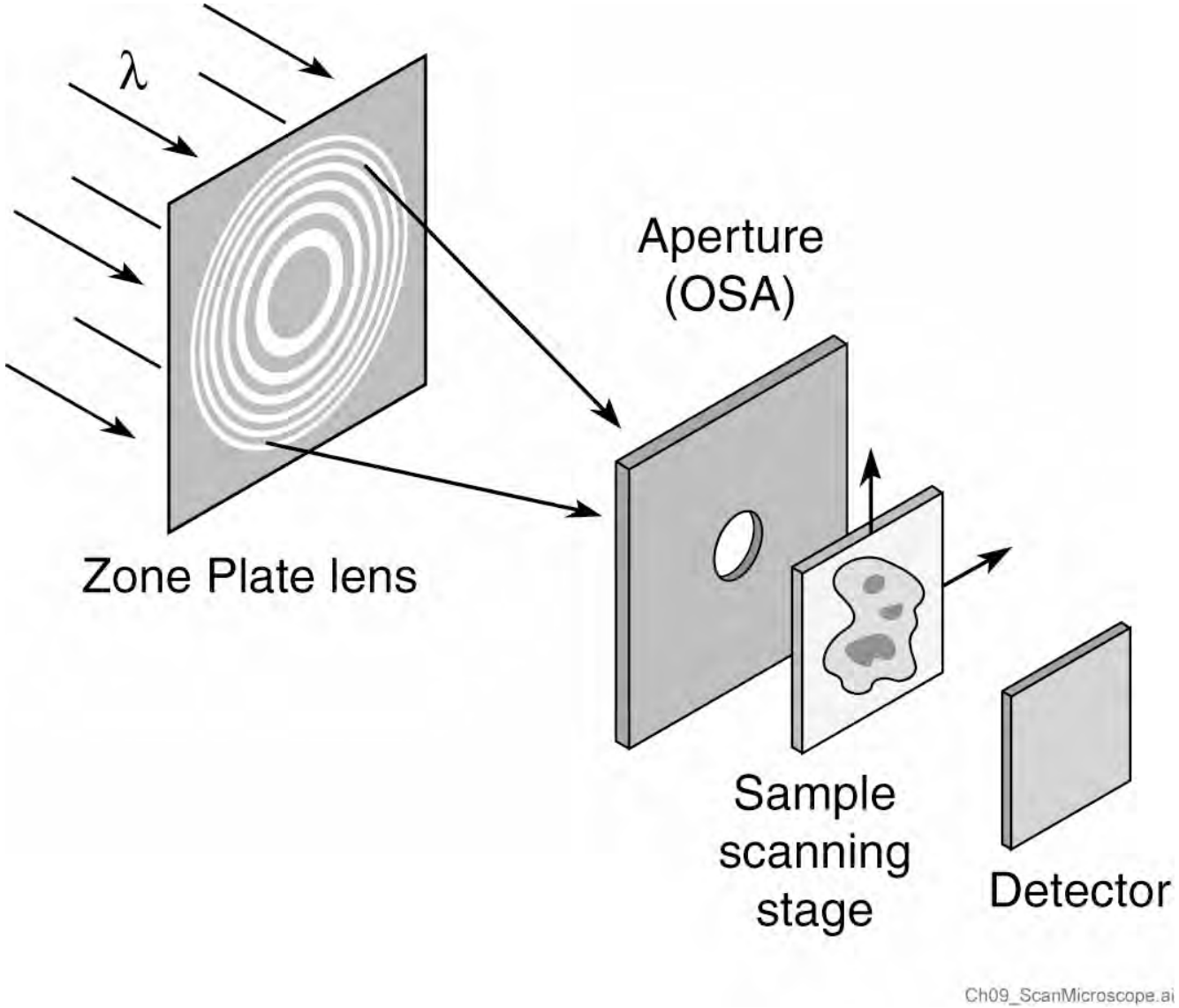

An Undulator Beamline for Scanning X-Ray Microscopy

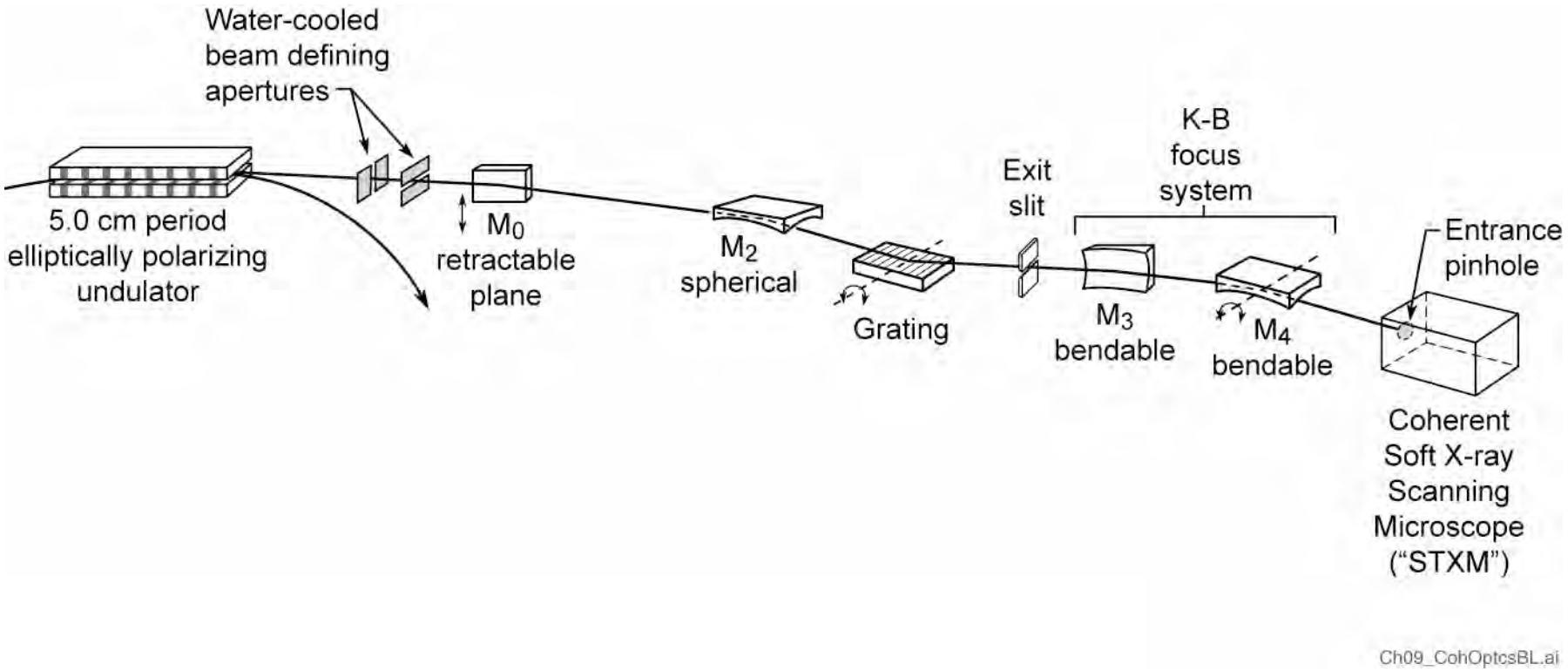

Coherent Power for an EPU at the ALS

U5 EPU

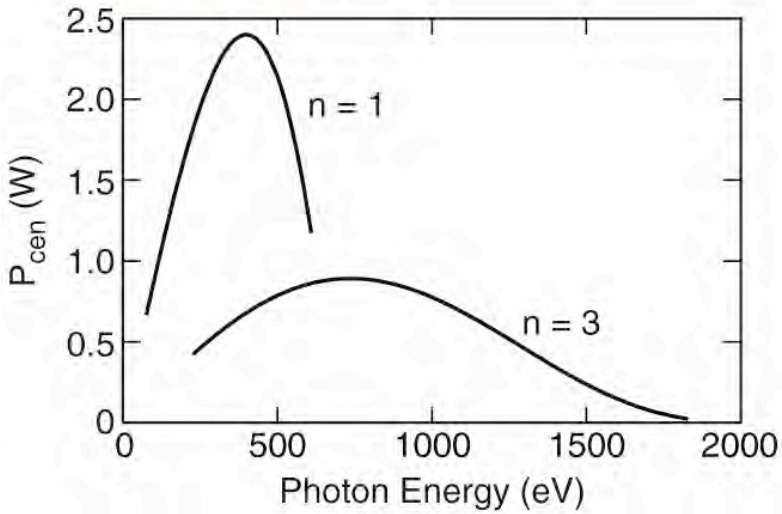

1.9 GeV, 400 mA
λ_u = 50 mm, N = 27
$0.5 \leq K \leq 4.0$
σ_x = 260 μm, σ_x' = 23 μr
σ_y = 16 μm, σ_y' = 3.9 μr
θ_{cen} = 61μr @ K = 0.87 (500 eV)

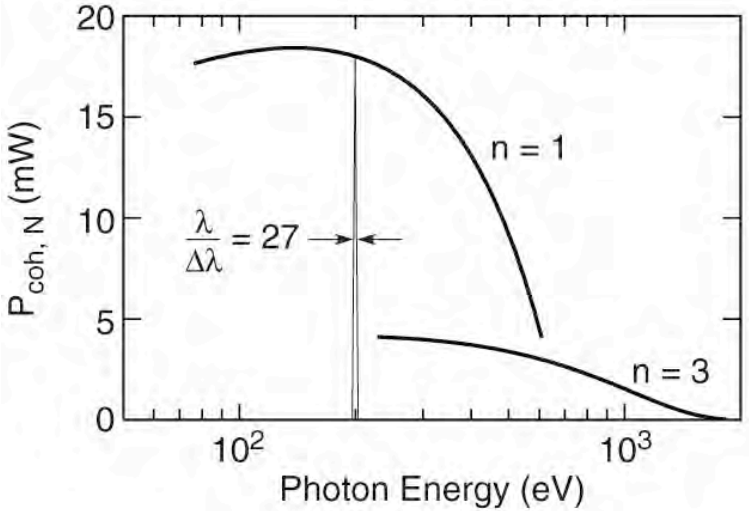

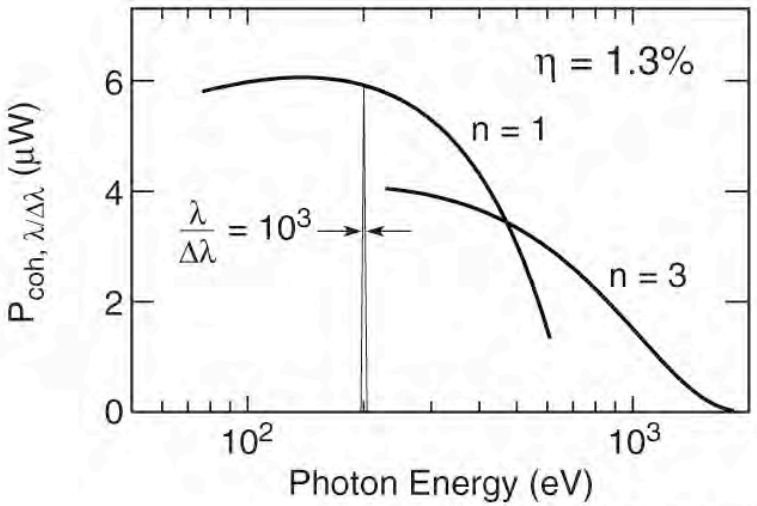

Ch08_ALS_U5epu_rev10.04.ai

Spectromicroscopy: High Spatial and High Spectral Resolution Studies of Surfaces and Thin Films

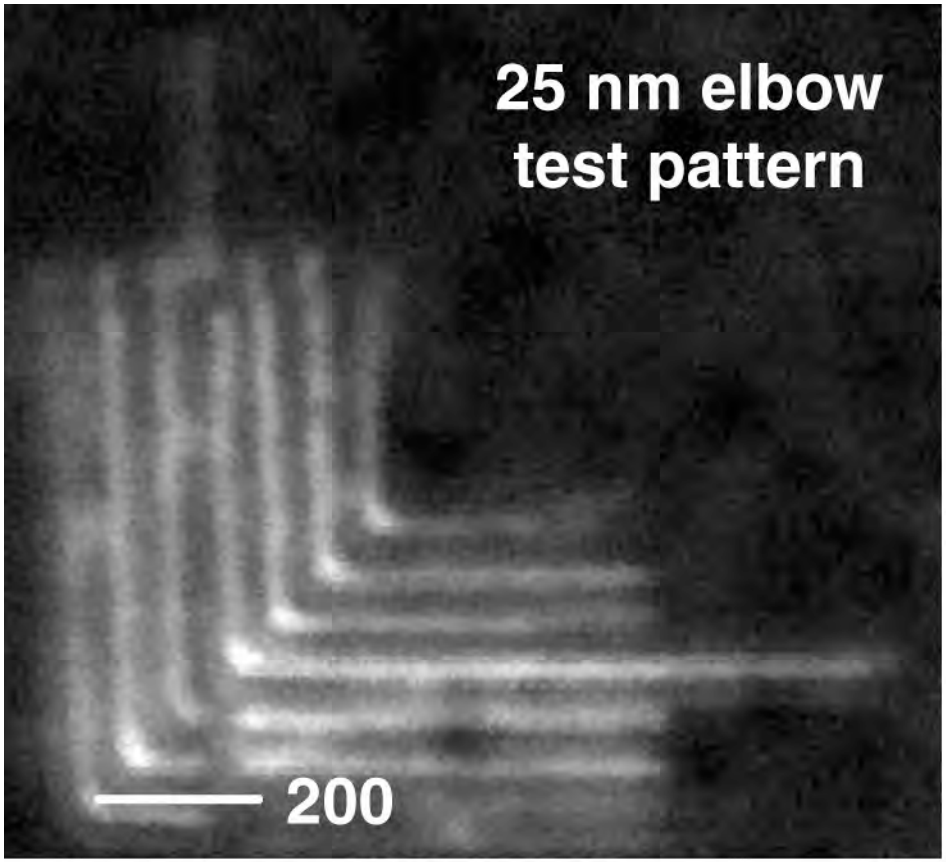

Scanning Soft X-Ray Microscope

ALS beamline 11.0.2
395 eV; $\lambda/\Delta\lambda \simeq 6000$
240×240 pixels
$1.2\ \mu m \times 1.2\ \mu m$
2 ms dwell time

Courtesy of Tolek Tyliszczak (Dec. 2003)

Ch09_Spectromicroscapy.ai

Biofilm from Saskatoon River

ALS-MES 11.0.2

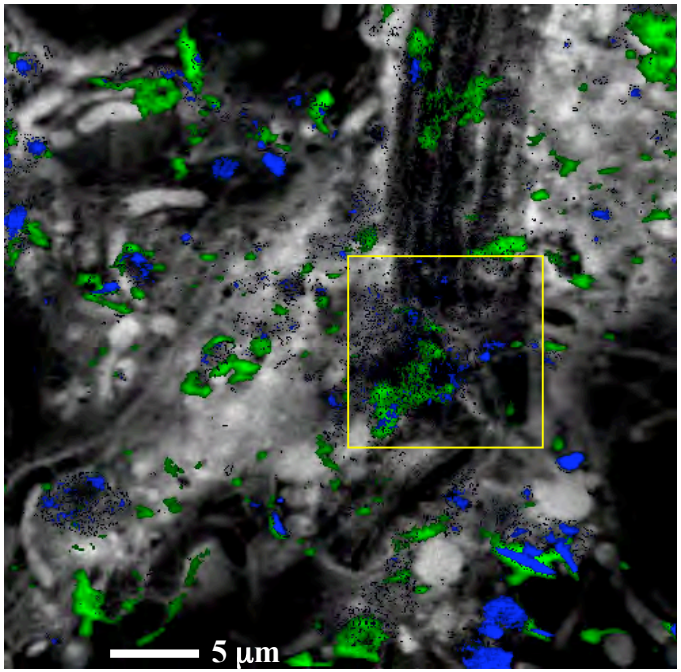

Protein (gray), Ca, K

RESULTS

•Ni, Fe, Mn, Ca, K, O, C elemental map,
(there was no sign of Cr.)
•Different oxidation states for Fe and Ni

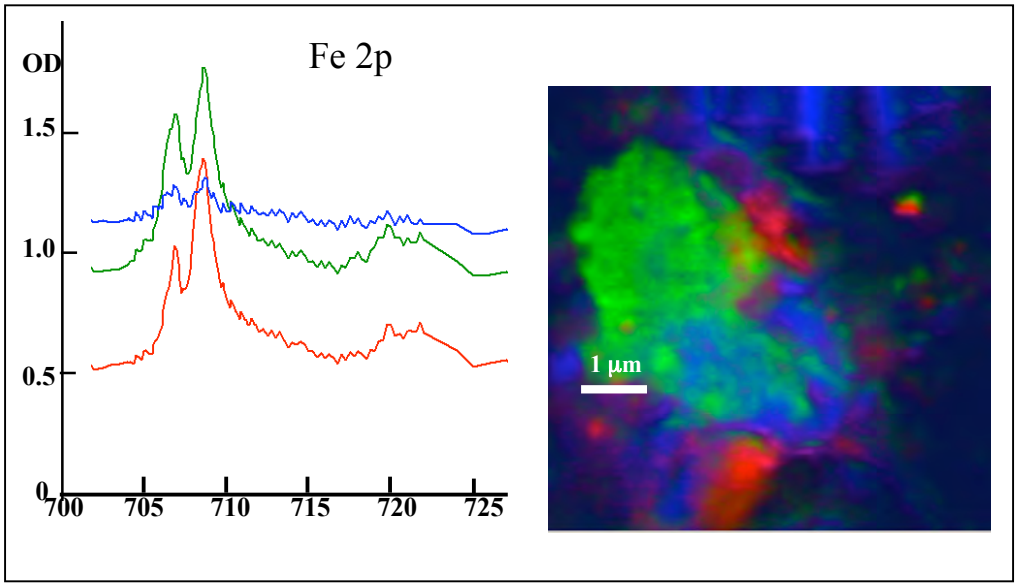

Different oxidation states (minerals) found for Fe & Ni

Tohru Araki, Adam Hitchcock (McMaster University)
Tolek Tyliszczak, LBNL
Sample from: John Lawrence, George Swerhone (NWRI-Saskatoon), *Gary Leppard* (NWRI-CCIW)

Patterned Polymer Photoresists

ALS-MES 11.0.2

M.K. Gilles, R. Planques, S.R. Leone
LBNL
Samples from B. Hinsberg, F. Huele
IBM Almaden

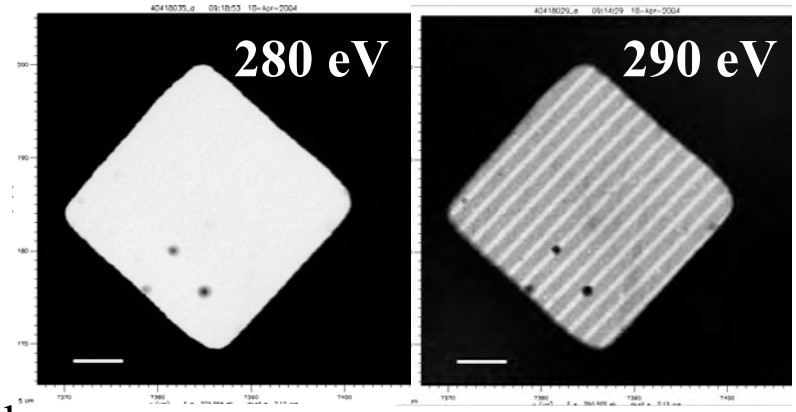

Exposure to UV light results in loss of carbonyl peak

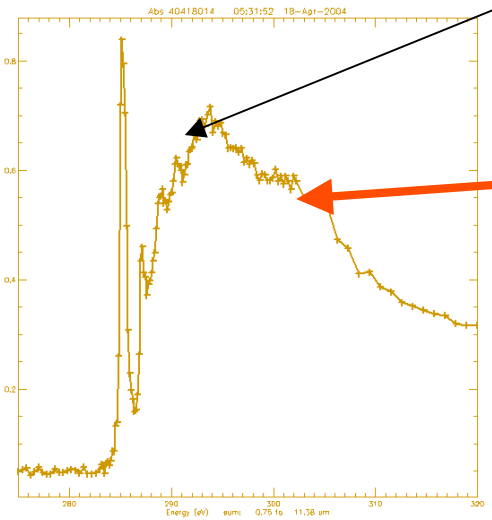

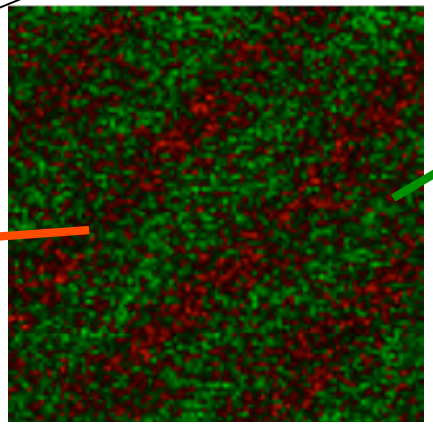

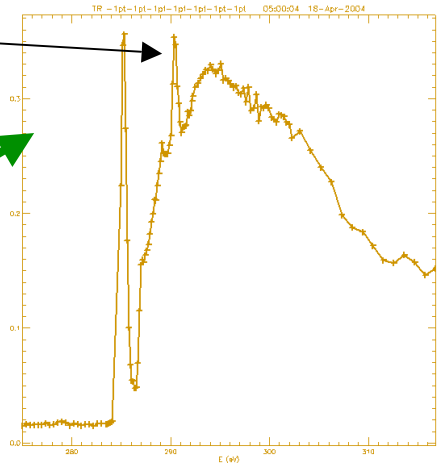

Map chemical spectra taken of pure samples
Onto a sample containing both components

Courtesy of Mary Gilles, LBNL

The Nanowriter: High Resolution Electron Beam Writing With High Placement Accuracy

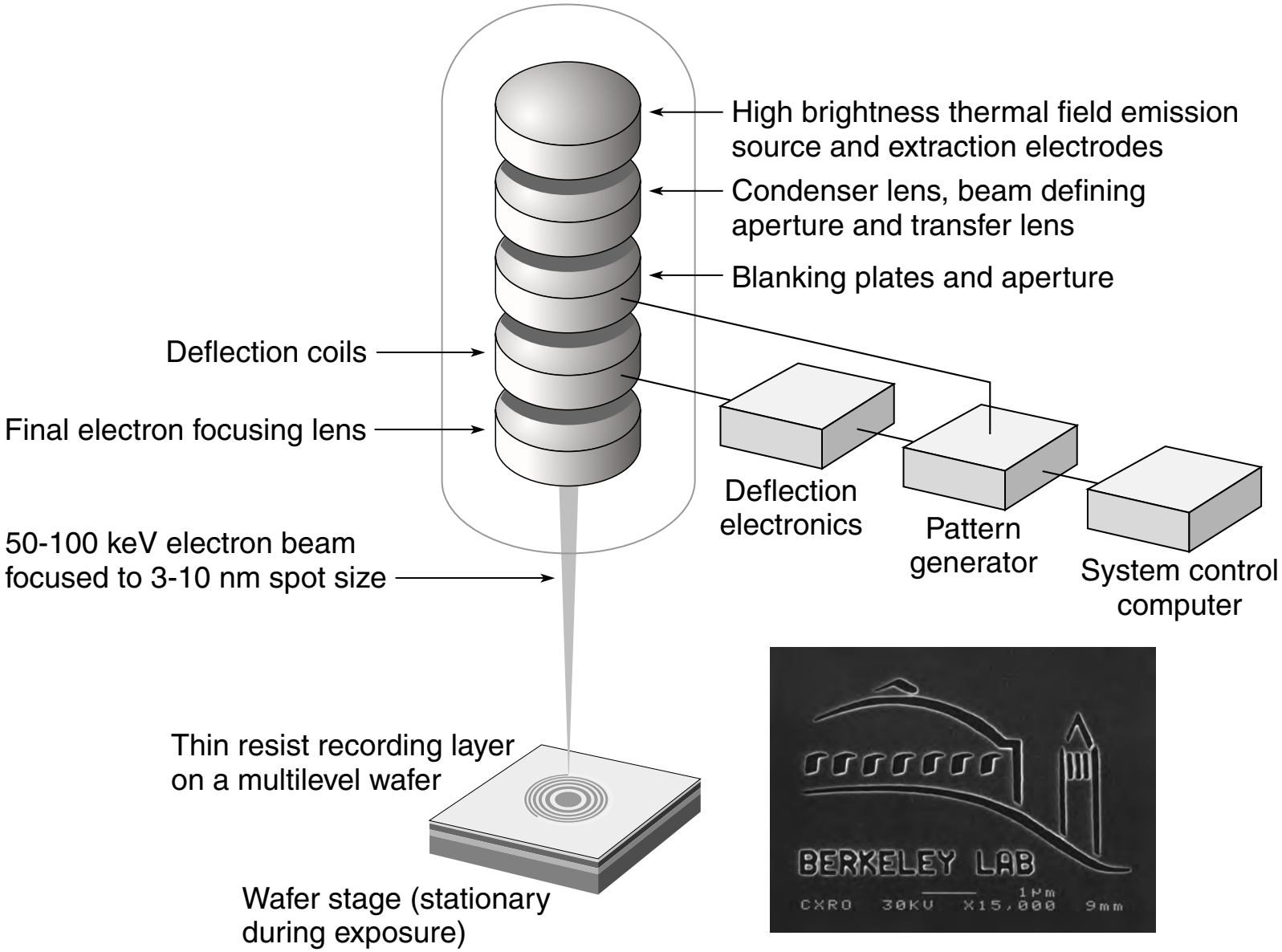

Courtesy of E. Anderson, LBNL

LBNL Nanowriter: Unique Ultra-high Resolution, High Accuracy Electron Beam Lithography Tool

Key Specifications

Parameter	Nanowriter
Beam size	5.0 nm 2.5 nm (New C3 lens)
Beam placement	2.5 nm (65 μm field) 20 nm (512 μm field)
Stitching	20 nm (1 cm field)
Beam voltage	20-100 kV
Beam current	1 nA at 10 nm 1.0-0.2 nA at 2.5 nm (new C3 lens)
Speed	25 MHz
Deflection field	16 bit
Interferometer	λ/1024
Wafer size	8"
Real time detection and feedback	Backscattered, transmitted and secondary electrons; digital image processing

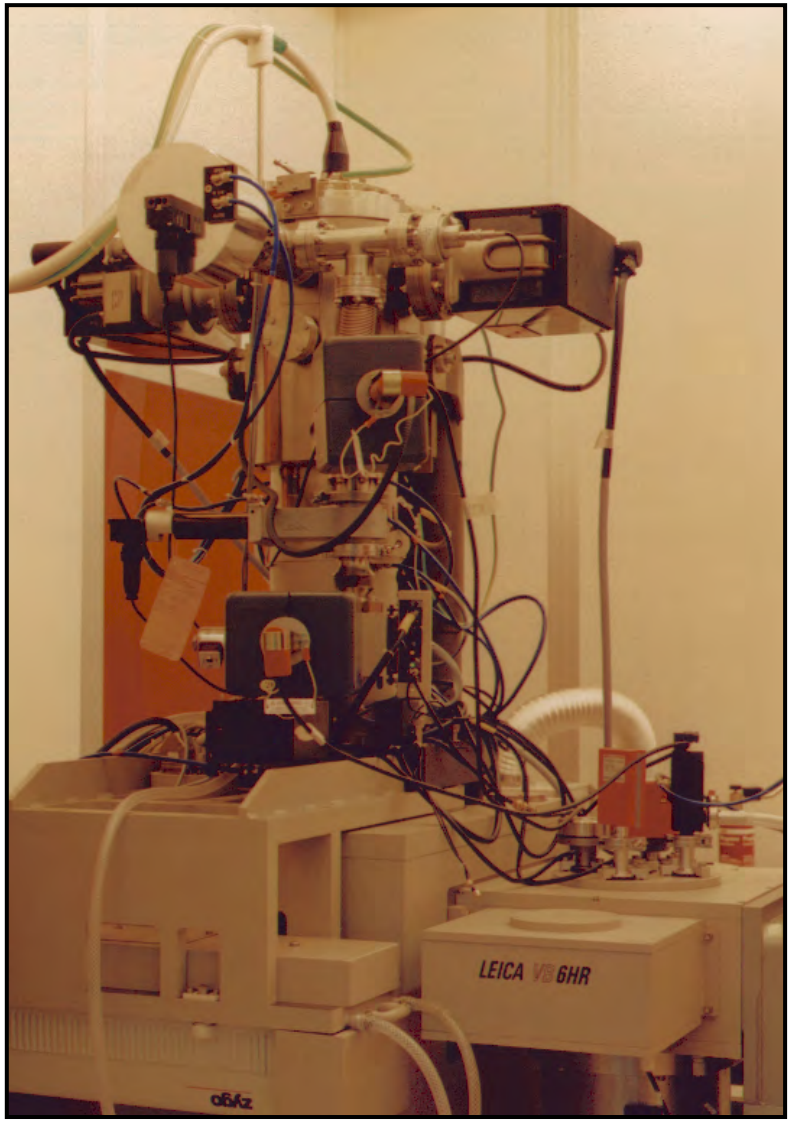

Courtesy of E. Anderson, LBNL

Nanofabrication is Critical for High Fidelity, High Aspect Ratio Zone Plates

1. Expose

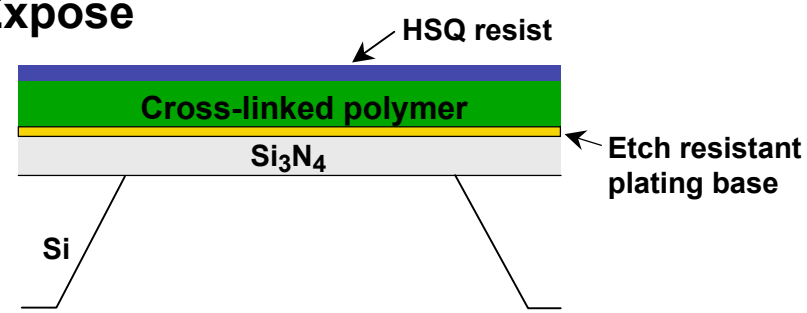

2. Develop

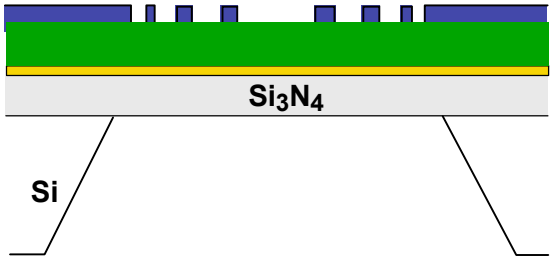

3. Cryogenic ICP Etch

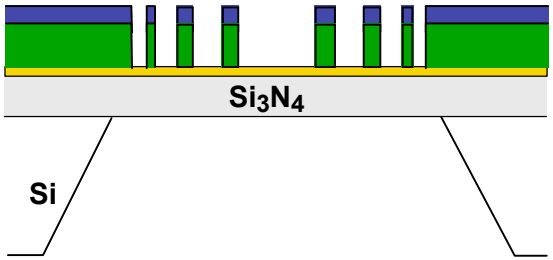

4. Plate

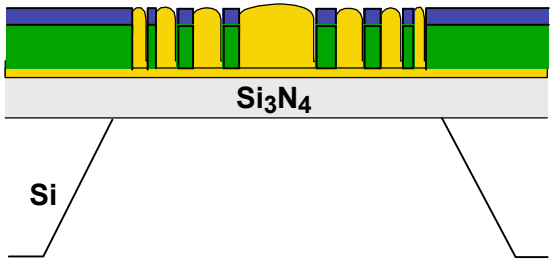

5. Strip Resist

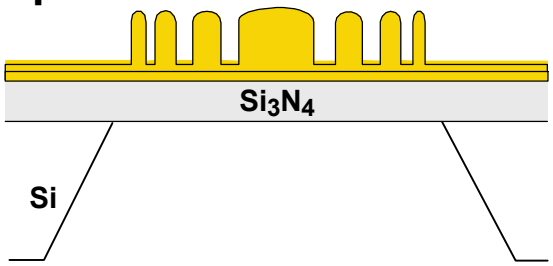

6. Strip Si_3N_4 and Cr/Au Plating Base

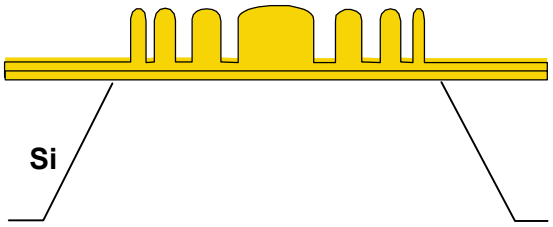

Courtesy of E. Anderson, A. Liddle, W. Chao, D. Olynick, and B. Harteneck (LBNL)